The Future of Snowstorms in Central and Eastern North America

Walker S. Ashley[a], Aaron Zeeb[b], Alex M. Haberlie[a], Vittorio A. Gensini[a], and Allison Michaelis[a]

[a] Department of Earth, Atmosphere, and Environment, Northern Illinois University, DeKalb, IL
[b] Department of Earth and Atmospheric Sciences, Central Michigan University, Mount Pleasant, MI

ORCID and email addresses:

Walker S. Ashley https://orcid.org/0000-0003-0816-3333 washley@niu.edu

Aaron W. Zeeb https://orcid.org/0009-0005-4519-9329 aaronwzeeb@gmail.com

Alex M. Haberlie https://orcid.org/0000-0001-9172-4028 ahaberlie1@niu.edu

Vittorio A. Gensini https://orcid.org/0000-0001-6362-9197 vgensini@niu.edu

Allison C. Michaelis https://orcid.org/0000-0002-0793-5779 amichaelis@niu.edu

Funding statement: This research was supported by the National Science Foundation Awards 1637225 and 1800582 and National Oceanic and Atmospheric Administration Award NA22OAR4690645.

Abstract

We investigate the changing snowstorm landscape in eastern North America using dynamically downscaled regional climate simulations that compare the late-twentieth century against mid- and late-twenty-first-century epochs for two climate pathways that include moderate and pessimistic warming. By identifying, tracking, and cataloging snowstorms, we illustrate how the frequency, snow water equivalent, and other features of these events may change. Results suggest changes in snowstorm characteristics are most significant for the pessimistic pathway, especially toward the late twenty-first century. There is similar event frequency between the historical period and mid-twenty-first-century projections but declines of 3 to 10% are still projected for snowstorm counts, hours, cumulative area, and snow water equivalent. By the late twenty-first century, snowstorm attributes have losses of 6 to 37% versus the historical period, revealing a projected acceleration in loss from the mid to late century. Spatially, snowstorm reduction is most dramatic along and south of the Ohio River Valley as the latitude that separates steady snowstorm counts to the north and reduced snowstorms to the south migrates poleward in the future. Similarly, extreme snowstorms decline to the south, with some northern regions experiencing increase in counts and snow water equivalent, affirming prior research theorizing that some snowfall may intensify as increasing moisture in a warming climate interacts with environments with temperatures still supportive of snowfall. Significant reductions in early and late cool-season snowstorms are projected across all future epochs, revealing a shrinking season. These results provide a set of perspectives on how a dominant cryospheric input—the snowstorm—will change across eastern North America in the future.

Keywords: Snow, snowstorm, United States, Canada, dynamical downscaling, climate change, climate models, climatology, extreme events

1. Introduction

Snowstorms produce a myriad of effects on the climate system, environment, and society, from impacts on hydrology and water storage, energy balance, agriculture, transportation, hydropower, sports and tourism, to snow-sensitive flora and fauna found in the extratropics. As the climate system undergoes change (IPCC 2021; USGCRP 2023), the timing, placement, and magnitude of snowstorms and their resulting snowfall and cover are evolving (Krasting et al., 2013; Diffenbaugh et al., 2013; Danco et al., 2016; Ashley et al., 2020). Considering the significance of snowstorms on natural and human systems, it is important to project how they may evolve in the future so that constituents impacted and dependent on this cryospheric input are informed of their potential change.

Prior climatological research on snow has focused on changes in snowfall (Knowles et al., 2006; Feng and Hu 2007; Krasting et al., 2013; Kapnick and Delworth 2013; O'Gorman 2014; Danco et al., 2016; Demaria et al., 2016), snowpack or mass (Dyer and Mote 2006; Notaro et al., 2014; Rhoades et al., 2017; Zeng et al., 2018; Pulliainen et al., 2020; Tedesche et al., 2023), and snow melt (Diffenbaugh et al., 2013; Mankin et al., 2015). Much of this work finds observed (Kunkel et al., 2009, 2016) and projected (Krasting et al., 2013; Lute et al., 2015; Ning and Bradley 2015; Demaria et al., 2016) declines in climatological snow metrics across North America, except for the most extreme snow days, which are predicted to have smaller fractional changes compared to mean snowfall in many regions (O'Gorman 2014; Janoski et al., 2018) and/or possibly intensify (Chen et al., 2020; Quante et al., 2021). Comparatively, little work has examined the primary drivers of climatological character of snow in the extratropics—the snowstorm—principally due to the challenges presented by observed data and classification of those data (Kunkel et al., 2013), as well as the relatively coarse resolution of GCMs or regional climate models (RCMs) used to project the future of these events that are driven by processes, and are most impactful, at the mesoscale (Suriano and Leathers 2015; Giorgi 2019; Gutowski et al., 2020). Most studies that have examined snow characteristics on shorter time scales have examined snow days (Danco et al., 2016; Janoski et al., 2018; Chen et al., 2020; Quante et al., 2021; McCray et al., 2023; Browne and Chen 2023) and not specific events, or storms, likely due to the difficulty in defining and tracking events, especially in relatively coarse model data that does not correspond to the scale needed to delineate storms (Ashley et al., 2020). However, recent work has explored the use of high-resolution RCMs to reveal the characteristics of snowstorms (Zarycki 2018; Ashley et al., 2020; Chen et al., 2021; McCray et al., 2023). Conclusions from these limited RCM efforts reveal broad declines in snowstorms and snow/precipitation ratios across the central and eastern CONUS.

Herein we employ a snowstorm tracking algorithm developed by Ashley et al. (2020) on high-resolution, dynamically downscaled RCM output to evaluate the potential change in these events in the central and eastern CONUS and adjacent parts of southern Canada for the twenty-first century. Specifically, we use the Gensini et al. (2023) simulations to explore how snowstorms in the mid- (2040–2055) and late- (2085–2100) twenty-first century compare to their late-twentieth-century (1990–2005) counterparts. Two greenhouse gas concentration trajectories representing intermediate and pessimistic climate pathways are explored for the twenty-first-century epochs, providing two perspectives on the future of snowstorms in North America. The novelty of this work compared to our prior effort (Ashley et al., 2020) is that the present study includes: a set of mid- and late-twenty-first-century simulations; intermediate and pessimistic climate pathways for each epoch; and the inclusion of thermodynamic as well as large-scale dynamic changes (i.e., changes in general circulation and modes of climate variability) to the climate system unlike a pseudo-global warming (PGW) approach (Liu et al., 2017; Ikeda et al., 2021; Chen et al., 2021; Chen et al., 2023; Brogli et al., 2023) that solely modifies the boundary conditions of a control RCM. Results reveal robust spatiotemporal changes in the characteristics of snowstorms across the domain under both climate projections. While computational, storage, and processing expenses generally limit RCM experiments, the RCM output and epoch comparisons herein provide an initial set of views on the potential changes of these impactful events, while also providing a structure for additional simulations and future research.

2. Data and methods

2.1 Data

We use dynamically downscaled RCM output generated by Gensini et al. (2023) to explore the changing snowstorm landscape in a domain that covers most of the central and eastern CONUS and adjacent parts of Canada (**Figure 1**). The Gensini et al. (2023) dataset was generated using bias-corrected output from NCAR's Community Earth System Model (CESM; Hurrel et al., 2013; Bruyère et al., 2014) CMIP phase 5 (CMIP5; Taylor et al., 2012) GCM as initial and lateral boundary conditions for WRF-ARW v.4.1.2 (Skamarock et al., 2019). Bias correction reduces errors produced by GCMs that, in turn, may be passed to WRF during the dynamical downscaling process, effectively improving performance and accuracy (Ines and Hansen 2006; Christensen et al., 2008; Gensini et al., 2023). The RCM was used in a convection-permitting configuration characterized by horizontal grid spacing of 3.75 km, 51 vertical levels, and data output intervals as frequent as 15 minutes. Gensini et al. (2023) refer to their RCM simulations as WRF-BCC (WRF-Bias Corrected CESM).

2.2 WRF-BCC verification

Gensini et al. (2023) compared the WRF-BCC historical 15-year period to Parameter-elevation Regressions on Independent Slopes Model (PRISM; Daly et al., 1994) and a gridded ensemble dataset based on 12,000 surface observation stations (Newman et al., 2015) to assess the potential temperature and precipitation bias in the simulations. Details of those comparisons and simulation verification are provided in Gensini et al. (2023), but are summarized as the following: The WRF-BCC closely recreated the spatial patterns of temperature and precipitation across the domain at monthly, seasonal, and annual timescales; biases included 2-m maximum temperature that were too cool across seasons and most locations, while an annual precipitation bias was generally restricted to the southeastern and eastern CONUS where WRF-BCC conditions were too dry; and, relevant for this study, simulations had a wet bias in the northern High Plains during the Dec-Feb period. Overall, monthly climatologies of temperature and precipitation found few locations that were outside of observational spread of uncertainty, providing confidence in the simulations' ability to replicate the historical climate.

To define and assess changes in snowstorms, we used the "AFWA_SNOW" variable generated from the Air Force Weather Agency (AFWA) diagnostics described in Creighton et al. (2014). AFWA_SNOW, which is the accumulation of liquid-equivalent snow, uses a precipitation type algorithm that is calculated at every model time step and is determined empirically, independent of the microphysics scheme. We compared the AFWA_SNOW variable—or, as we label, WRF-BCC snow water equivalent (SWE)—against NOAA National Operational Hydrologic Remote Sensing Center's SNOw Data Assimilation System (SNODAS) data (Barret 2003; NSDIC 2024). Assimilating both remote sensing and in situ data, SNODAS has several snow variables—including SWE—that are used to provide the best possible modeled estimates of snow cover in support of simulations and analysis (NSDIC 2024). Daily SNODAS SWE output for October 1–April 1 2003–2013 were used as for comparison with daily HIST WRF-BCC output for 1990–2005 (**Figure 2**). While years do not overlap wholly since SNODAS data only exist since 2003, this comparative analysis provides a perspective on the validity of WRF-BCC output for the historical period. Annual SWE means for SNODAS and WRF-BCC were generated, with absolute difference values between the two datasets used to express similarities, differences, and possible biases. We caution that SNODAS is a model dataset and not "ground truth" since there is immense difficulty and uncertainty—or, as McCrary et al. (2022) describe, insufficiency—in snow observations and accurately representing snow derived variables such as SWE. The considerable uncertainties of snow in assimilated and simulation datasets are well described and illustrated in Clow et al. (2012) and McCrary et al. (2017, 2022).

The percentage difference illustrates that the areal SWE mean totals from WRF-BCC are generally representative of the assimilated SNODAS dataset, especially in climatologically high-SWE regions. There is strong agreement between the datasets in the central and northern Great Plains, Midwest, Ohio Valley, Mid-Atlantic, and, to a lesser extent, the Northeast and upper Great Lakes; in the latter two regions, WRF-BCC contains a low SWE bias. In regions where snow is rare—generally along and south of 35ºN parallel, and especially along the far southern gradient of areas that experience snow—there are larger percentage differences, similar to the difference found between SNODAS and Liu et al. (2017) PGW simulation SWE output evaluated in Ashley (2020). In these southern regions, snow is relatively rare, illustrated by the order of magnitude difference in SWE compared to regions to the north. The rarity, low magnitude (<10 mm SWE annually), and intermittent spatial variability of snowstorms in this region, especially for relatively short 15-year epochs, are likely causes of these seemingly large differences. Further, differences in how SNODAS and WRF-BCC are derived and their sensitivity to very small SWE accumulations could be an additional reason for the disparities. Despite these apparent biases, the objective of this study is to generate and compare deltas—or "apples to apples" comparison—between WRF-BCC epochs, not to uncover reasonings and provide corrections for SWE between SNODAS and the Gensini et al. (2023) simulations.

2.3 Snowstorm tracking methods

This research employs the same snowstorm-tracking algorithm described in Ashley et al. (2020) and provided by Haberlie (2020). Algorithm details and schematic examples are provided in Ashley et al. (2020; cf. their Extended data Fig. 2) and are summarized herein. The algorithm uses SWE output, which provides a reasonable representation of spatial distribution and intensity of snow. We do not use snow accumulation proxies in the algorithm due to the variability in snow-to-liquid ratios, which are highly dynamic spatially and temporally across both seasons and individual storm events (Baxter et al., 2005).

Initially, the algorithm detects 3-hourly "slices" of potential snow events, where a slice is a collection of connected grid points that meet or exceed 0.1 mm of SWE for a 3-hr period that is greater than ~100 km^2. Slices are concatenated to produce a "swath" and, thereafter, tested for spatiotemporal overlap to assure the representation of a spatial outline of a potential snow event. All swath, or snow-event, candidates are further tested to confirm that the first and last slices in the concatenated swath have an area of at least 1 X 10^5 km^2 and exceed 24 hours between the first and last slice. These swaths are considered snow events and are tracked across a domain that includes most of the central and eastern CONUS and adjacent regions of Canada that are roughly less than 1500 m elevation east of the Continental Divide. Some meso-β and γ events may not be captured by the algorithm purposely; this includes lake-effect snow cases that are not affiliated with migratory extratropical cyclones across the Great Lakes (Ashley et al., 2020) and do not meet the spatial criterion minimum.

The historical epoch (HIST; 1990–2005) is compared against two future periods that are characterized by RCP 4.5 and 8.5, which represent intermediate and pessimistic anthropogenic climate change trajectories, respectively. The two future epochs include mid-twenty-first-century (MID; 2040–2055) and end-of-twenty-first-century (EOC; 2085–2100) projections.

Like Ashley et al. (2020), we calculated the 50^{th} and 90^{th} percentiles for 3-hour SWE accumulations for the HIST period. These were calculated by gathering all HIST pixels greater than or equal to 0.1 mm within the tracked snowstorms across the central and eastern CONUS domain during the October–April period. The HIST 50^{th} and 90^{th} percentile values, representing moderate and extreme snowfall intensities, are 0.35 mm and 1.18 mm, respectively. These serve as thresholds for comparing historical conditions to future epochs to assess whether these intensities occur more frequently in a changing climate. We also compare the totality of SWE across the domain for monthly and seasonal periods to assess how the ratio of snow-to-total precipitation may potentially change.

Statistical significance tests are performed on counts and means between HIST and respective future epochs using the Mann-Whitney U test with a p-value of less than 0.05. We caution that confidence in these significance tests is relatively low due to small sample size between epochs (n = 15) and may be influenced by interannual variability as much as, or more than, anthropogenic climate change (McCray et al., 2023) and difficulty in quantifying uncertainty due to a singular RCM approach (McCrary et al., 2017; McCrary and Mearns 2019; McCrary et al., 2022). Similarly, percentage change calculations may be influenced by small sample size, which is a common issue for current convective permitting RCM experiments.

3. Results

3.1 Changes in cumulative snowstorm attributes

All four future epochs are projected to have fewer cool-season snowstorms than HIST, which averaged 78.4 seasonal events across the domain with a maximum of 94 and minimum of 60 events per season during the 15-year epoch (**Figure 3a, Table S1**). The percent change differences in mean counts are relatively small for MID4.5 (-5.19%), MID8.5 (-9.18%), and EOC4.5 (-8.9%) but robust for EOC8.5 (-26.7%); both 8.5 projections, as well as the EOC4.5, are significantly different from HIST. The percentage decline in EOC8.5 is similar to Ashley et al. (2020), who found a decline of 28% snowstorms in Liu et al.,'s (2017) PGW simulations, which compared similar time periods and used the same RCP. Visualizing changes with another perspective, seasonal cumulative frequency of snowstorms reveals large overlap with a slight decrease between midcentury RCPs compared to HIST, but with increasing spread and significant reduction in events toward the end of the century compared to HIST (**Figure 4a-b**).

SWE also declines across all future epochs (**Figure 3b**), but there is considerable central tendency overlap and relatively small percentage change differences for MID4.5 (-3.0%), MID8.5 (-7.7%), and EOC4.5 (-6.0%). Only the EOC8.5 is significantly different than HIST, with a nearly 32% reduction in SWE, or roughly 227 km^3 reduction in mean seasonal domain SWE compared to HIST's 715 km^3; this percentage change is nearly the same for that found in Ashley et al. (2020). The character of these trends is further revealed using seasonal cumulative SWE (**Figure 4d-e**), with notable overlap in SWE for midcentury between epochs and a modest decline for EOC4.5 and significant decline of EOC8.5 compared to HIST. A similar declining pattern from HIST to future epochs is found for other snowstorm attributes, including seasonal cumulative snowstorm swath spatial extent, or area, and swath hours (**Figure 3c-d**). The most notable attribute change is cumulative snowstorm area, which has percent change declines ranging from 6.7% for MID4.5 to roughly 10% for both MID8.5 and EOC4.5 to a robust, and significantly different, reduction of 37.2% for EOC8.5. Though varying, the overall decline in these attributes suggests that the reduction in SWE is caused by fewer snowstorms and, collectively, smaller snowstorm footprints.

3.2 Spatial changes

Consistent with the overall snowfall climatology (Durre et al., 2013), there is a strong latitudinal gradient in snowstorm events across the domain (**Figure 1**). All epochs illustrate a snowstorm maximum in southeast Canada, with more than 32 snowstorm tracks per season—or, on average, 1.2 storms a week—from the northern Great Lakes to Hudson Bay, generally north of the St. Lawrence River. Equatorward from this maximum, the northern CONUS Plains through the Northeast experience 16 to 32 events per season, with a slowly waning frequency toward the Mid-South, where less than one event per season is expected. Snowstorm climatology is consistent with the overall maximum in extratropical cyclones, which drive most winter precipitation events (Hawcroft et al., 2012) across the domain (Plante et al., 2014; Lombardo et al., 2015; Eichler 2020).

Future epochs versus HIST generally show declining snowstorm counts (**Figure 5 and 6**) and SWE (**Figures 7 and 8**) across the domain, especially across the central and northern CONUS Plains—consistent with GCM-based research that has shown a decrease in future blizzards in this region (Browne and Chen 2023)—and some parts of the Tennessee and southern Ohio River Valleys, Cumberland Plateau, into the Mid-Atlantic. There are a few areas of slight increase in snowstorm frequency and SWE in MID4.5, MID8.5, and EOC4.5. The most dramatic spatial change is found in EOC8.5, where snowstorm frequency is found to decline 25 to 50% across most areas that experience events (**Figure 6b,d**). Across all epochs, the southern fringe of the domain—from Texas to the southern Mid-Atlantic—may see a near removal of snowstorms in the future, which is consistent with the expected increasing temperatures under future anthropogenic climate change scenarios (Almazroui et al., 2021; Gensini et al., 2023 (cf. their Fig. 8b); USGCRP 2023) affecting those events that have lower tropospheric and surface temperatures that are marginal to produce winter precipitation (Krasting et al., 2013; Liu et al., 2016; Danco et al., 2016). The trend toward more rain-dominated or transitional (rain and snow) precipitation climate regimes along the equatorward edge of regions that experience snow, which is leading to an overall poleward shift in snow-affected areas, has already been established in observed data over the last 40 years (Tedesche et al., 2023); WRF-BCC projections suggest that this trend will continue.

3.3 Seasonal, monthly, and weekly changes

Similar to Ashley et al. (2020), the greatest temporal change in the character of snowstorms across the domain occurs during the shoulder seasons (**Table S1, Figures 4c,f**) where temperatures, as discussed, are generally marginal to produce snowfall and the partition of snowfall-to-rainfall is susceptible to warming due to interannual variability and anthropogenic climate change (Huntington et al., 2004; Knowles et al., 2006; Feng and Hu 2007; Krasting et al., 2013; Danco et al., 2016; Chen et al., 2020; Prein and Heymsfield 2020; Shi and Liu et al., 2021). Though overall numbers are low, the early-season month of October has notable decreases in event counts, ranging from -26.2% for MID4.5 to -80.1% for EOC8.5. Similar, but generally smaller, percentage change departures in snowstorm counts from HIST are found for November, March, and April. Interestingly, January has notable percent change departures for all future epochs—ranging from -7.3% to -10.2%; conversely, December and February reveal little departure in percent changes in snowstorm counts. Broadly, the percent changes in snowstorm counts for future epochs versus HIST are found in other snowstorm attributes, including total SWE, cumulative swath hours, and cumulative swath area. The latter attribute, though variable, shows the greatest percent change, suggesting that the extent of snowstorm footprints will be smaller in the future under most scenarios and months.

Providing another perspective, weekly-calculated percent changes of snowstorm counts, SWE, and snowstorm area for future epochs versus HIST reveal the dramatic change in the shoulder seasons, with many weekly departures for MID4.5 and MID8.5 exceeding -40% and EOC4.5 and EOC8.5 exceeding -60% (**Figure 9**). The most notable change in the character of the season is found in EOC8.5, with a significant departure in percent change found across the entire season except in late February and parts of March. Overall, these results suggest a shortening of the snowstorm season, which is consistent with prior research that has examined daily snowfall using GCMs (Danco et al., 2016; Chen et al., 2020).

3.4 Changes in moderate and intense areas of accumulation

Research using GCMs and relatively coarse RCMs suggests that there may be smaller fractional changes, or even increases, in future intense, or heavy, snowfall days in regions where mean seasonal snowfall is projected to broadly decrease (O'Gorman 2014; Danco et al., 2016; Chen et al., 2020; Quante et al., 2021; McCray et al., 2023). This dichotomy is likely due to climate warming leading to more rain than snow when thermal conditions are marginal (McCray et al., 2023), whereas slight decreases or increases in extreme snowfalls may be due to increasing moisture (i.e., specific humidity) in environments with temperatures still supportive of snowfall (O'Gorman 2014; Quante et al., 2020) and/or shifting storm tracks and intensification of extratropical cyclones projected across parts of the domain (Colle et al., 2013; Eichler 2020; Browne and Chen 2023). O'Gorman (2014, 2015) theorizes that extreme snowfall situations occur in a range of temperatures that are, for the most part, insensitive to warming temperatures due to anthropogenic climate change.

To assess the more intense areas in swaths identified and tracked in this study, we gathered SWE pixels within each swath that exceeded the HIST 50th and 90th percentiles for 3-hour accumulations (cf. Extended data Fig. 2 in Ashley et al. (2020)); these percentiles represent the spatial extent of moderate and extreme intensities within each corresponding swath, respectively, and provide a point of comparison to studies that have examined extremes using daily snowfalls from GCM or coarse RCM output. WRF-BCC's high spatial and temporal resolution is particularly suited for this analysis since it can resolve banded, meso-β snow events (Novak et al., 2004; Baxter and Schumacher 2017; McCrary 2022) driven by low-to-mid-level frontogenesis (Novak et al., 2008, 2010; Ganetis et al., 2018) that are responsible for high snowfall rates and notable impacts to society (Changnon and Changnon 2011).

Overall, various measures of central tendency for total SWE, accumulated area, and duration for both 50th and 90th SWE percentile events for MID and EOC have small declines or broad overlap with HIST, except for RCP 8.5 (**Figure 10**). Percentage changes between 50th SWE percentile events for future epochs and HIST generally show small decreases of 4 to 9% for 50th percentile swath counts except for EOC8.5, which decreased by nearly 24% (**Table S2**). Percentage changes for 90th SWE percentile swath counts are mixed, with slight increases or decreases, except for, again, EOC8.5 (**Table S3**). This percentage change pattern for 50th and 90th SWE percentiles is generally replicated for other variables such as total SWE, accumulated area, and duration. Beyond the significantly different RCP 8.5 scenarios, the relative overlap across all variables suggests that changes in moderate and intense events will be subtle; though, some of this overlap between HIST and the future epochs is likely caused by the capturing of deltas across the entirety of the domain. Latitudinally, these changes appear more robust (**Figures 11 and 12**).

In related manner, spatially, the most pronounced change signal in both the MID and EOC epochs versus HIST are across the southern part of the domain, where both 50th and 90th percentile events have notable declines, which is consistent with the trend found for overall snowstorm counts. There is a sharp gradient to the changes in moderate and extreme events, which moves poleward during the EOC climate pathways. There are regions of increase in extreme events poleward of the relative sharp gradient of increase/decrease in these events. Percent change increases are most prominent in the 90th percentile compared to the 50th percentile and overall snowstorm counts. This finding suggesting that climate warming induces more rain than snow in areas to the south with marginal thermal profiles supportive of snow, while increasing moisture in a warming climate (Held and Soden 2006; Willett et al., 2007; Lombardo et al., 2015; Coffel et al., 2018) leads to enhanced snowfall rates and more extreme events where temperatures remain sufficient for snowfall production to the immediate north. Spatially, this finding corresponds with the O'Gorman (2014, 2015) theory discussed above and reinforced by others (Krasting et al., 2013; Danco et al., 2016; Chen et al., 2020; Quante et al., 2021; McCray et al., 2023).

3.5 Changes in snow/precipitation ratio

Prior research suggests that the ratio of snowfall to overall precipitation across most of North America has decreased during the last century (Feng and Hu 2007; Shi and Liu 2021) and is projected to continue to decrease in the twenty-first century (Räisänen 2008; Krasting et al., 2013). We use these prior results as a basis to examine the change in the fraction of liquid equivalent that falls as snow in the Gensini et al. (2023) simulations during the cool season (**Figure 13**).

Roughly 14.7% of the October through April liquid-equivalent precipitation across the domain is snow in the HIST epoch. By mid-century, the percentage of precipitation that falls as snow drops to 14.2% under the intermediate scenario (3.3% percent change from HIST) and 13.8% under the pessimistic scenario (6.6% percent change). By the end of the century, the percentage decreases to 13.4% for intermediate (8.6% percent change from HIST) and 9.6% for pessimistic (34.3% percent change) scenarios. Though the EOC8.5 is the only change that is significantly different from the historical epoch, the proportion of precipitation that falls as snow during the cool season is, on average, projected to decrease across all future epochs. Monthly, the EOC epochs reveal the largest decreases in that proportion of precipitation that is snow, with significant decreases compared to HIST for all months for EOC8.5. Projected MID changes are mixed, but most months still show declines in the snow-to-total-precipitation ratio.

Spatially, the percentage contribution of snow to the overall cool-season precipitation, as expected, reveals a strong latitudinal gradient, with the highest SWE contributions—exceeding 60% in HIST—across the northern Plains into the Great Lakes (**Figure 14**). Percentage changes in snow contribution to overall precipitation from HIST to MID are projected to be variable across the study domain; broad declines are interspersed with some local increases. Significantly different changes in SWE contributions for the MID epochs are restricted to areas off the Mid-Atlantic and Northeast coast and intermittent parts of the Great Plains (**Figure 15**). Percent contribution differences for the EOC epochs are more notable, with significant decreases far more widespread than MID, with nearly the entirety of the domain that experiences snow expected to have statistically significant declines in the snow-to-total-precipitation ratio in the EOC8.5 scenario.

The snow-rain partitioning is driven by thermodynamic changes in the climate system, with broad increases in surface and lower tropospheric temperatures leading to changes in the precipitation that falls as snow due to higher melting layer heights (Feng and Hu 2007; Lemke et al., 2007; Räisänen 2008; Krasting et al., 2013; Almazroui et al., 2021; Gensini et al., 2024). This is particularly the case for regions that have temperatures marginal for snowfall and, temporally, during the shoulder, or transition, months (Knowles et al., 2006; Krasting et al., 2013). Per the Clausius-Clapeyron relationship (Trenberth et al., 2003; Pall et al., 2007), as temperatures increase, higher evaporation rates lead to greater atmospheric moisture available for snowstorms and, therefore, higher precipitation rates and extremes (Donat et al., 2016; Lee et al., 2021). Therefore, regions that retain surface and tropospheric temperatures suitable for snow may see minimal decreases, or even slight increases, in snow totals and extremes (O'Gorman 2014; Quante et al., 2020).

4. Discussion and conclusion

Snowfall and related accumulations produce considerable impacts to society and modify energy and hydrologic cycles. Assessing how snow will evolve under future climates is essential for understanding changes in the earth-atmospheric system, environment, and society. While it is established that anthropogenic climate change will modify and likely intensify precipitation events (IPCC 2021; USGCRP 2023), how snow will change in a future climate state is complex as snow is particularly attuned to subtle—and difficult to gauge—changes in lower tropospheric and surface temperatures that must be sufficient to produce snow at the ground (O'Gorman 2015).

Even though overall snowfall and snow-to-total-precipitation ratios may decrease in future due to a warming climate (Diffenbaugh et al., 2013; Kapnick and Delworth 2013; Krasting et al., 2013; Notaro et al., 2014; McCrary et al., 2022; McCray et al., 2023), high-end events may not decrease at the same rate as mean seasonal snowfall and may shift climatologically poleward (O'Gorman 2014; McCray et al., 2023). This persistence and/or even enhancement of heavy daily snowfalls is theorized to occur because of the increasing availability of moisture in a warming climate that overlaps an optimal temperature range (~-4 to -2ºC) for extreme snowfall (O'Gorman 2014, 2015; Quante et al., 2021; McCray et al., 2023). Conversely, research by Browne and Chen (2023) suggests that blizzard-like events may decline in the Northern Plains and Upper Midwest and Ashley et al. (2020) project significant decreases in the frequency and size of snowstorms, including intense storms under a pessimistic climate pathway. Adding to the complexity, projections suggest that extratropical cyclones that produce a majority of central and eastern CONUS snowfall (Hawcroft et al., 2012) may, on the mean, intensify and shift poleward (McDonald 2010; Tamarin-Brodsky and Kaspi 2017; Hawcroft et al., 2018; Eichler 2020); though, other research suggests a reduction in cyclone numbers across North America (Catto et al., 2011), but dichotomous intensity results (Priestley and Catto 2022). Unquestionably, the changing snow landscape across North America is complex and uncertain.

Our work complements the limited body of research that has focused on the primary producer of snowfall and snowpack: the snowstorm. This method differs from most research on the topic, which has generally employed daily or longer periods to measure and evaluate changes in snowfall using coarse GCMs or ~12-25 km grid spacing RCMs (Notaro et al., 2014; O'Gorman 2014; Danco et al., 2016; Janoski et al., 2018; Zarzycki 2018; Chen et al., 2020; Quante et al., 2021; McCray 2023). Our use of an RCM at 3.75 km grid spacing permits the capturing of meso-β snow bands within storms that are frequently the cause of significant accumulations (Novak et al., 2004; Changnon and Changnon 2011; Baxter and Schumacher 2017; McCrary 2022), resolves important physiographic and orographic effects, and enables the identification, tracking, and cataloging of snowstorms at high spatiotemporal resolution (Ashley et al., 2020). Further, we used a non-PGW method to promote the inclusion of both thermodynamic and large-scale dynamic changes to the climate system and explore two separate climate pathways for mid- and late-twenty-first-century periods.

Our results reveal that the frequency, placement, and intensity of snowstorms are projected to change across the central and eastern CONUS and adjacent regions of southern Canada during the twenty-first century. Changes are most dramatic for the pessimistic climate pathway toward the end-of-the-twenty-first century, where significant declines are projected for various snowstorm attributes, including frequency, SWE, area, and duration. Mid-twenty-first-century changes for all epochs and climate pathways are more muted, but all snowstorm variables still show average percent change declines of 3 to 10% from the HIST epoch. The two most notable changes in all future epochs are the significant declines in shoulder season snowstorms and the poleward shift in the latitude that demarcates steady snowstorm counts to the north and reduced, or elimination of, snowstorms to the south. The latter occurs with moderate (50^{th} percentile SWE) and intense (90^{th} percentile SWE) events, as well, with intense events illustrating areas of increase poleward of the sharp drop off in snowstorms along and south of the Arkansas, Tennessee, and Ohio River Valleys. This lack of decline and, in some regions, increases in high-end events reaffirms results from prior research by O'Gorman (2014) and McCray et al. (2023). The partitioning of snow and rain is projected to change, with the ratio of snow to total precipitation across the study domain expected to decline from 13.4% to 34.3% by the end of the twenty-first century. Such changes have implications for energy and moisture budgets, water storage and balance, flood risk, and, overall, environmental and societal systems dependent on water.

Our research, while providing an initial set of perspectives on the changing snowstorm landscape, has several limitations. The narrow ensemble envelope (RCP 4.5 and 8.5) and relatively short period of record in each epoch (15 years) constrains explanatory power and retains uncertainty when examining extreme events. With such short temporal windows, fully assessing the individual and collective contribution of large-scale climate modes and variability (e.g., Ghatak et al., 2010; Liu et al., 2015, 2020) versus anthropogenic climate change to the alterations uncovered is unknown. While expansion of scenarios and analysis periods is always desirable, computing resources, data storage, data egress, and post-processing are restrictive. As these constraints ease in the future as computational and storage capabilities improve, research groups and programs should collectively strive to increase the RCM populations by exploring variations in grid spacing, model physics and parameterization schemes, dynamical cores, additional GCM inputs and shared socioeconomic pathways, bias corrections, and perturbations during model initialization (Gensini 2021; Ashley et al., 2023). This ensemble framework will improve explanatory power and reduce uncertainty in our understanding of snowstorms and how they change in the future (McCray et al., 2023).

Acknowledgements

This research was supported by the National Science Foundation Awards 1637225 and 1800582 and National Oceanic and Atmospheric Administration Award NA22OAR4690645. The authors acknowledge high-performance computing support from Cheyenne (doi:10. 5065/D6RX99HX) provided by NCAR's Computational and Information Systems Laboratory, sponsored by the National Science Foundation. We also acknowledge the high-performance computing support from Comet, which was hosted by the San Diego Supercomputer Center at the University of California, San Diego. This computational resource was made available by the Atmospheric River Program (Phases 2 and 3), which is supported by the California Department of Water Resources (awards 4600013361 and 4600014294, respectively) and the U.S. Army Corps of Engineers Engineer Research and Development Center (award USACE W912HZ-15-2-0019). We also acknowledge and thank Dr. Michael Papka (ANL) for data storage and postprocessing assistance. This research used resources of the Argonne Leadership Computing Facility, which is a DOE Office of Science User Facility supported under Contract DE-AC02-06CH11357. We thank the editor and reviewers for their constructive feedback.

Conflict of Interest statement

The authors declare no conflicts of interest.

Data availability statement

The source code for the snow event identification and tracking is available from Haberlie (2020) and/or https://github.com/ahaberlie/FutureSnow. In the spirit of reproducibility, if an email request is made to the authors, we will make available data and materials necessary to interested researchers for duplication and verification of results herein. WRF-BCC simulation output is available in netCDF format and stored on Argonne systems. We request that anyone interested in using the WRF-BCC output contact coauthor Gensini (vgensini@niu.edu) for information on how to access the data, including any collaboration.

Supporting Information

Table S1. Mean monthly and seasonal total snowstorm counts and percentage changes for all epochs. Percentage changes are calculated for each future epoch versus HIST.

Table S2. As in Table S1, except for 50th percentile events.

Table S3. As in Table S1, except for 90th percentile events.

References

Almazroui, M., M. N. Islam, F. Saeed, and Coauthors, 2021: Projected changes in temperature and precipitation over the United States, Central America, and the Caribbean in CMIP6 GCMs. *Earth Syst. Environ.*, **5**, 1–24, https://doi.org/10.1007/s41748-021-00199-5.

Ashley, W. S., A. M. Haberlie, and V. Gensini, 2020: Reduced frequency and size of late twenty-first-century snowstorms over North America. *Nat. Climate Change*, **10**, 539-544.

Barrett, A., 2003: National Operational Hydrologic Remote Sensing Center Snow Data Assimilation System (SNODAS) products at NSIDC. NSIDC Special Report 11, National Snow and Ice Data Center, https://nsidc.org/sites/nsidc.org/files/files/nsidc_special_report_11.pdf

Baxter, M. A., and P. N. Schumacher, 2017: Distribution of single-banded snowfall in central U.S. cyclones. *Wea. Forecasting*, **32**, 533–554, https://doi.org/10.1175/WAF-D-16-0154.1.

Baxter, M. A., C. E. Graves, and J. T. Moore, 2005: A Climatology of Snow-to-Liquid Ratio for the Contiguous United States. *Wea. Forecasting*, **20**, 729–744, https://doi.org/10.1175/WAF856.1.

Brogli, R., and Coauthors, 2023: A global model of climate-driven water scarcity including the feedbacks of water use and adaptation dynamics. *Geosci. Model Dev.*, **16**, 907–926, https://doi.org/10.5194/gmd-16-907-2023.

Browne, A., and L. Chen, 2023: Investigating the occurrence of blizzard events over the contiguous United States using observations and climate projections. *Environ. Res. Lett.*, **18**, 114044, https://doi.org/10.1088/1748-9326/ad0449.

Catto, J. L., L. C. Shaffrey, and K. I. Hodges, 2011: Northern Hemisphere Extratropical Cyclones in a Warming Climate in the HiGEM High-Resolution Climate Model. *J. Climate*, **24**, 5336–5352, https://doi.org/10.1175/2011JCLI4181.1.

Changnon, S. A., and D. Changnon, 2005: Snowstorm catastrophes in the United States. *Global Environ. Change Part B: Environ. Hazards*, **6**, 158–166, https://doi.org/10.1016/j.hazards.2006.06.001.

Chen, G., W. Wang, C. Cheng, and H. Hsu, 2021: Extreme snow events along the coast of the Northeast United States: Potential changes due to global warming. *J. Climate*, **34**, 2337–2353, https://doi.org/10.1175/JCLI-D-20-0197.1.

Chen, H., J. Sun, and W. Lin, 2020: Anthropogenic influence would increase intense snowfall events over parts of the Northern Hemisphere in the future. *Environ. Res. Lett.*, https://doi.org/10.1088/1748-9326/abbc93.

Chen, X., L. R. Leung, Y. Gao, and Coauthors, 2023: Sharpening of cold-season storms over the western United States. *Nat. Clim. Chang.*, **13**, 167–173, https://doi.org/10.1038/s41558-022-01578-0.

Christensen, J. H., F. Boberg, O. B. Christensen, and P. Lucas-Picher, 2008: On the need for bias correction of regional climate change projections of temperature and precipitation. *Geophys. Res. Lett.*, **35**, L20709, https://doi.org/10.1029/2008GL035694.

Clow, D. W., L. Nanus, K. L. Verdin, and J. Schmidt, 2012: Evaluation of SNODAS snow depth and snow water equivalent estimates for the Colorado Rocky Mountains, USA. *Hydrol. Process.*, **26**, 2583–2591.

Creighton, G., E. Kuchera, R. Adams-Selin, J. McCormick, S. Rentschler, and B. Wickard, 2014: AFWA diagnostics in WRF.

Coffel, E. D., R. M. Horton, and A. de Sherbinin, 2018: Temperature and humidity-based projections of a rapid rise in global heat stress exposure during the 21st century. *Environ. Res. Lett.*, **13**, 014001, https://doi.org/10.1088/1748-9326/aaa00e.

Colle, B. A., Z. Zhang, K. A. Lombardo, E. Chang, P. Liu, and M. Zhang, 2013: Historical Evaluation and Future Prediction of Eastern North American and Western Atlantic Extratropical Cyclones in the CMIP5 Models during the Cool Season. *J. Climate*, **26**, 6882–6903, https://doi.org/10.1175/JCLI-D-12-00498.1.

Daly, C., R. P. Neilson, and D. L. Phillips, 1994: A statistical-topographic model for mapping climatological precipitation over mountainous terrain. *J. Appl. Meteorol. Climatol.*, **33**, 140–158.

Danco, J. F., A. M. DeAngelis, B. K. Raney, and A. J. Broccoli, 2016: Effects of a warming climate on daily snowfall events in the Northern Hemisphere. *J. Climate*, **29**, 6295–6318, https://doi.org/10.1175/JCLI-D-15-0687.1.

Demaria, E. M. C., J. K. Roundy, S. Wi, and R. N. Palmer, 2016: The effects of climate change on seasonal snowpack and the hydrology of the Northeastern and Upper Midwest United States. *J. Climate*, **29**, 6527–6541, https://doi.org/10.1175/JCLI-D-15-0632.1.

Diffenbaugh, N. S., M. Scherer, and M. Ashfaq, 2012: Response of snow-dependent hydrologic extremes to continued global warming. *Nat. Clim. Change*, **3**, 379–384.

Donat, M., A. Lowry, L. Alexander, and Coauthors, 2016: More extreme precipitation in the world's dry and wet regions. *Nature Clim. Change*, **6**, 508–513, https://doi.org/10.1038/nclimate2941.

Durre, I., M. F. Squires, R. S. Vose, X. Yin, A. Arguez, and S. Applequist, 2013: NOAA's 1981–2010 U.S. climate normals: Monthly precipitation, snowfall, and snow depth. *J. Appl. Meteor. Climatol.*, **52**, 2377–2395, https://doi.org/10.1175/JAMC-D-13-051.1.

Dyer, J. L., and T. L. Mote, 2006: Spatial variability and trends in observed snow depth over North America. *Geophys. Res. Lett.*, **33**(16), L16503, https://doi.org/10.1029/2006GL027258.

Eichler, T. P., 2020: The impacts of a warming climate on winter mid-latitude cyclones in the NARCCAP model suite. *Clim. Dyn.*, **54**, 4379–4398, https://doi.org/10.1007/s00382-020-05236-z.

Feng, S., and Q. Hu, 2007: Changes in winter snowfall/precipitation ratio in the contiguous United States. *J. Geophys. Res. Atmos.*, **112**(D15), D15109, https://doi.org/10.1029/2007JD008397.

Ganetis, S. A., B. A. Colle, S. E. Yuter, and N. P. Hoban, 2018: Environmental conditions associated with observed snowband structures within northeast U.S. winter storms. *Mon. Wea. Rev.*, **146**, 3675–3690, https://doi.org/10.1175/MWR-D-18-0054.1.

Gensini, V. A., 2021: Severe convective storms in a changing climate. *Climate Change and Extreme Events*, A. Fares, Ed., Springer, 39–56, https://doi.org/10.1016/C2019-0-04922-9.

Gensini, V., A. Haberlie, and W. S. Ashley, 2023: Convection-permitting simulations of historical and possible future climate over the contiguous United States. *Clim. Dyn.*, **60**, 109–126.

Gensini, V. A., W. S. Ashley, A. C. Michaelis, and A. M. Haberlie, J. Goodin, and B. C. Wallace, 2024: Hailstone size dichotomy in a warming climate. *npj Clim. Atmos. Sci.*, **7**, 185, https://doi.org/10.1038/s41612-024-00728-9.

Ghatak, D., G. Gong, and A. Frei, 2010: North American Temperature, Snowfall, and Snow-Depth Response to Winter Climate Modes. *J. Climate*, **23**, 2320–2332, https://doi.org/10.1175/2009JCLI3050.1.

Giorgi, F., 2019: Thirty years of regional climate modeling: Where are we and where are we going next? *J. Geophys. Res. Atmos.*, **124**, 6881–6904, https://doi.org/10.1029/2018JD030094.

Gutowski, W. J., and Coauthors, 2020: The ongoing need for high-resolution regional climate models: Process understanding and stakeholder information. *Bull. Amer. Meteor. Soc.*, **101**, E664–E683, https://doi.org/10.1175/BAMS-D-19-0113.1.

Haberlie, A. M., 2020: ahaberlie/Future_Snow. Zenodo, (https://doi.org/10.5281/zenodo.3674139

Hawcroft, M., E. Walsh, K. Hodges, and G. Zappa, 2018: Significantly increased extreme precipitation expected in Europe and North America from extratropical cyclones. *Environ. Res. Lett.*, *13*, 12, https://doi.org/10.1088/1748-9326/aae8e0.

Hawcroft, M. K., L. C. Shaffrey, K. I. Hodges, and H. F. Dacre, 2012: How much Northern Hemisphere precipitation is associated with extratropical cyclones? *Geophys. Res. Lett.*, **39**, L24708, https://doi.org/10.1029/2012GL053866.

Held, I. M., and B. J. Soden, 2006: Robust Responses of the Hydrological Cycle to Global Warming. *J. Climate*, **19**, 5686–5699, https://doi.org/10.1175/JCLI3990.1.

Huntington, T. G., G. A. Hodgkins, B. D. Keim, and R. W. Dudley, 2004: Changes in the proportion of precipitation occurring as snow in New England (1949–2000). *J. Climate*, **17**, 2626–2636, https://doi.org/10.1175/1520-0442(2004)017<2626>2.0.CO;2.

Ikeda, K., Rasmussen, R., Liu, C. *et al.,* Snowfall and snowpack in the Western U.S. as captured by convection permitting climate simulations: current climate and pseudo global warming future climate. *Clim Dyn* **57**, 2191–2215 (2021). https://doi.org/10.1007/s00382-021-05805-w

Ines, A. V. M., and J. W. Hansen, 2006: Bias correction of daily GCM rainfall for crop simulation studies. *Agric. For. Meteor.*, **138**, 44–53, https://doi.org/10.1016/j.agrformet.2006.03.009.

IPCC, 2021: *Climate Change 2021: The Physical Science Basis*. Contribution of Working Group I to the Sixth Assessment Report of the Intergovernmental Panel on Climate Change [Masson-Delmotte, V., P. Zhai, A. Pirani, S. L. Connors, C. Péan, S. Berger, N. Caud, Y. Chen, L. Goldfarb, M. I. Gomis, M. Huang, K. Leitzell, E. Lonnoy, J. B. R. Matthews, T. K. Maycock, T. Waterfield, O. Yelekçi, R. Yu, and B. Zhou (eds.)]. Cambridge University Press, Cambridge, United Kingdom and New York, NY, USA, In press, https://doi.org/10.1017/9781009157896.

Janoski, T. P., A. J. Broccoli, S. B. Kapnick, and N. C. Johnson, 2018: Effects of Climate Change on Wind-Driven Heavy-Snowfall Events over Eastern North America. *J. Climate*, **31**, 9037–9054, https://doi.org/10.1175/JCLI-D-17-0756.1.

Kapnick, S. B., and T. L. Delworth, 2013: Controls of global snow under a changed climate. *J. Climate*, **26**, Krasting, J. P., A. J. Broccoli, K. W. Dixon, and J. R. Lanzante, 2013: Future Changes in Northern Hemisphere Snowfall. *J. Climate*, **26**, 7813–7828, https://doi.org/10.1175/JCLI-D-12-00832.1.

Knowles, N., M. D. Dettinger, and D. R. Cayan, 2006: Trends in snowfall versus rainfall in the western United States. *J. Climate*, **19**, 4545–4559.

Kunkel, K. E., M. Palecki, L. Ensor, K. G. Hubbard, D. Robinson, K. Redmond, and D. Easterling, 2009: Trends in Twentieth-Century U.S. Snowfall Using a Quality-Controlled Dataset. *J. Atmos. Oceanic Technol.*, **26**, 33–44, https://doi.org/10.1175/2008JTECHA1138.1.

Kunkel, K. E., D. A. Robinson, S. Champion, and Coauthors, 2016: Trends and extremes in Northern Hemisphere snow characteristics. *Curr. Clim. Change Rep.*, **2**, 65–73, https://doi.org/10.1007/s40641-016-0036-8.

Lee, J.-Y., J. Marotzke, G. Bala, et al.,, 2021: Future global climate: Scenario-based projections and near-term information. *Climate Change 2021: The Physical Science Basis. Contribution of Working Group I to the Sixth Assessment Report of the Intergovernmental Panel on Climate Change*, V. Masson-Delmotte, and Coauthors, Eds., Cambridge University Press, 553–672, https://doi.org/10.1017/9781009157896.006.

Liu, C., K. Ikeda, R. Rasmussen, M. Barlage, et al.,, 2017: Continental-scale convection-permitting modeling of the current and future climate of North America. *Climate Dyn.*, **49**, 71–95, https://doi.org/10.1007/s00382-016-3327-9.Lombardo, K., B. A. Colle, and Z. Zhang, 2015: Evaluation of Historical and Future Cool Season Precipitation over the Eastern United States and Western Atlantic Storm Track Using CMIP5 Models. *J. Climate*, **28**, 451–467, https://doi.org/10.1175/JCLI-D-14-00343.1.

Liu, Z., X. He, W. Ma, and Y. Wang, 2020: Robust increases in extreme Pacific North American events under greenhouse warming. *Geophys. Res. Lett.*, **47**, e2019GL086309, https://doi.org/10.1029/2019GL086309.

Liu, Z., Z. Jian, K. Yoshimura, N. H. Buenning, C. J. Poulsen, and G. J. Bowen, 2015: Recent contrasting winter temperature changes over North America linked to enhanced positive Pacific-North American pattern. *Geophys. Res. Lett.*, **42**, 7750–7757.

Lute, A. C., J. T. Abatzoglou, and K. C. Hegewisch, 2015: Projected changes in snowfall extremes and interannual variability of snowfall in the western United States. *Water Resour. Res.*, *51*, 960–972.

Mankin, J., D. Viviroli, D. Singh, A. Hoekstra, and N. Diffenbaugh, 2015: The potential for snow to supply human water demand in the present and future. *Environ. Res. Lett.*, **10**, 114016.

McCray, C. D., G. A. Schmidt, D. Paquin, M. Leduc, Z. Bi, M. Radiyat, C. Silverman, M. Spitz, and B. R. Brettschneider, 2023: Changing nature of high-impact snowfall events in Eastern North America. *J. Geophys. Res. Atmos.*, **128**, https://doi.org/10.1029/2023JD038804.

McCrary, R. R., and L. O. Mearns, 2019: Quantifying and diagnosing sources of uncertainty in midcentury changes in North American snowpack from NARCCAP. *J. Hydrometeor., 20*, 2229-2252, https://doi.org/10.1175/JHM-D-18-0248.1.

McCrary, R. R., S. McGinnis, and L. O. Mearns, 2017: Evaluation of Snow Water Equivalent in NARCCAP Simulations, Including Measures of Observational Uncertainty. *J. Hydrometeor.*, **18**, 2425–2452, https://doi.org/10.1175/JHM-D-16-0264.1.

McCrary, R. R., L. O. Mearns, M. Hughes, S. Biner, and M. S. Bukovsky, 2022: Projections of North American snow from NA-CORDEX and their uncertainties, with a focus on model resolution. *Climatic Change*, *170*, 20, https://doi.org/10.1007/s10584-021-03294-8.

McDonald, R. E., 2010: Understanding the impact of climate change on Northern Hemisphere extra-tropical cyclones. *Clim. Dyn.*, **37**, 1399–1425, https://doi.org/10.1007/s00382-010-0916-x.

Newman, A. J., and Coauthors, 2015: Gridded ensemble precipitation and temperature estimates for the contiguous U.S. *J. Hydrometeorol.*, **16**, 2481–2500.

Ning, L., and R. S. Bradley, 2015: Snow occurrence changes over the central and eastern United States under future warming scenarios. *Sci. Rep.*, **5**, 17073, https://doi.org/10.1038/srep17073.

Notaro, M., D. Lorenz, C. Hoving, and M. Schummer, 2014: Twenty-First-Century Projections of Snowfall and Winter Severity across Central-Eastern North America. *J. Climate*, **27**, 6526–6550, https://doi.org/10.1175/JCLI-D-13-00520.1.

Novak, D. R., B. A. Colle, and S. E. Yuter, 2008: High-resolution observations and model simulations of the life cycle of an intense mesoscale snowband over the northeastern United States. *Mon. Wea. Rev.*, **136**, 1433–1456, https://doi.org/10.1175/2007MWR2233.1.

Novak, D. R., B. A. Colle, and A. R. Aiyyer, 2010: Evolution of mesoscale precipitation band environments within the comma head of northeast U.S. cyclones. *Mon. Wea. Rev.*, **138**, 2354–2374, https://doi.org/10.1175/2010MWR3219.1.

Novak, D. R., L. F. Bosart, D. Keyser, and J. S. Waldstreicher, 2004: An observational study of cold season–banded precipitation in northeast U.S. cyclones. *Wea. Forecasting*, **19**, 993–1010, https://doi.org/10.1175/815.1.

NSIDC, 2024: Data Assimilation System (SNODAS) Data Products at NSIDC, Version 1. National Snow and Ice Data Center, https://doi.org/10.7265/N5TB14TC.

O'Gorman, P. A., 2014: Contrasting responses of mean and extreme snowfall to climate change. *Nature*, **512**, 416–418.

O'Gorman, P. A., 2015: Precipitation extremes under climate change. *Curr. Clim. Change Rep.*, *1*, 49–59, https://doi.org/10.1007/s40641-015-0009-3.

Pall, P., M. R. Allen, and D. A. Stone, 2006: Testing the Clausius–Clapeyron constraint on changes in extreme precipitation under CO_2 warming. *Clim. Dyn.*, **28**, 351–363.

Parsons, D. B., 2003: The changing character of precipitation. *Bull. Amer. Meteor. Soc.*, **84**, 1205–1218, https://doi.org/10.1175/BAMS-84-9-1205.

Plante, M., S.-W. Son, E. Atallah, J. Gyakum, and K. Grise, 2014: Extratropical cyclone climatology across eastern Canada. *Int. J. Climatol.*, **34**, 3035–3050, https://doi.org/10.1002/joc.4170.

Prein, A. F., and A. J. Heymsfield, 2020: Increased melting level height impacts surface precipitation phase and intensity. *Nat. Clim. Change*, **10**, 771–776, https://doi.org/10.1038/s41558-020-0825-x.

Prein, A. F., and Coauthors, 2017: Continental-scale convection permitting modeling of the current and future climate of North America. *Clim. Dyn.*, **49**(1–2), 71–95, https://doi.org/10.1007/s00382-016-3327-9.

Priestley, M. D. K., and J. L. Catto, 2022: Future changes in the extratropical storm tracks and cyclone intensity, wind speed, and structure. *Weather Clim. Dyn.*, **3**, 337–357, https://doi.org/10.5194/wcd-3-337-2022.

Pulliainen, J., K. Luojus, C. Derksen, and Coauthors, 2020: Patterns and trends of Northern Hemisphere snow mass from 1980 to 2018. *Nature*, **581**, 294–298, https://doi.org/10.1038/s41586-020-2258-0.

Quante, L., S. N. Willner, R. Middelanis, and Coauthors, 2021: Regions of intensification of extreme snowfall under future warming. *Sci. Rep.*, **11**, 16621, https://doi.org/10.1038/s41598-021-95979-4.

Räisänen, J., 2008: Warmer climate: Less or more snow? *Climate Dynamics*, **30**, 307–319, https://doi.org/10.1007/s00382-007-0289-y.

Rhoades, A. M., P. A. Ullrich, and C. M. Zarzycki, 2018: Projecting 21st century snowpack trends in western USA mountains using variable-resolution CESM. *Clim. Dyn.*, **50**, 261–288, https://doi.org/10.1007/s00382-017-3606-0.

Shi, S., and G. Liu, 2021: The latitudinal dependence in the trend of snow event to precipitation event ratio. *Sci. Rep.*, **11**, 18112, https://doi.org/10.1038/s41598-021-97451-9.

Suriano, Z. J., and D. J. Leathers, 2015: Twenty-first century snowfall projections within the eastern Great Lakes region: Detecting the presence of a lake-induced snowfall signal in GCMs. *Int. J. Climatol.*, **36**, 4583–4602, https://doi.org/10.1002/joc.4488.

Tamarin-Brodsky, T., and Y. Kaspi, 2017: Enhanced poleward propagation of storms under climate change. *Nature Geosci.*, **10**, 908–913, https://doi.org/10.1038/s41561-017-0001-8.

Tedesche, M., T. Dahl, and J. Giovando, 2023: Changing snow regime classifications across the contiguous United States. *Authorea Preprints*, https://doi.org/10.22541/essoar.167340718.86199797/v1.Trenberth, K. E., A. Dai, R. M. Rasmussen, and

USGCRP, 2023: *Fifth National Climate Assessment*. A. R. Crimmins, C. W. Avery, D. R. Easterling, K. E. Kunkel, B. C. Stewart, and T. K. Maycock, Eds. U.S. Global Change Research Program, Washington, DC, USA, https://doi.org/10.7930/NCA5.2023.

Willett, K. M., N. P. Gillett, P. D. Jones, and P. W. Thorne, 2007: Attribution of observed surface humidity changes to human influence. *Nature*, **449**, 710–712, https://doi.org/10.1038/nature06207.

Zarycki, C., 2018: Projecting Changes in Societally Impactful Northeastern U.S. Snowstorms. *Geophys. Res. Lett.*, **45**(12), 67–75, https://doi.org/10.1029/2018GL079820.

Zeng, X., P. Broxton, and N. Dawson, 2018: Snowpack change from 1982 to 2016 over conterminous United States. *Geophys. Res. Lett.*, **45**(23), 12,940–12,947, https://doi.org/10.1029/2018GL079621.

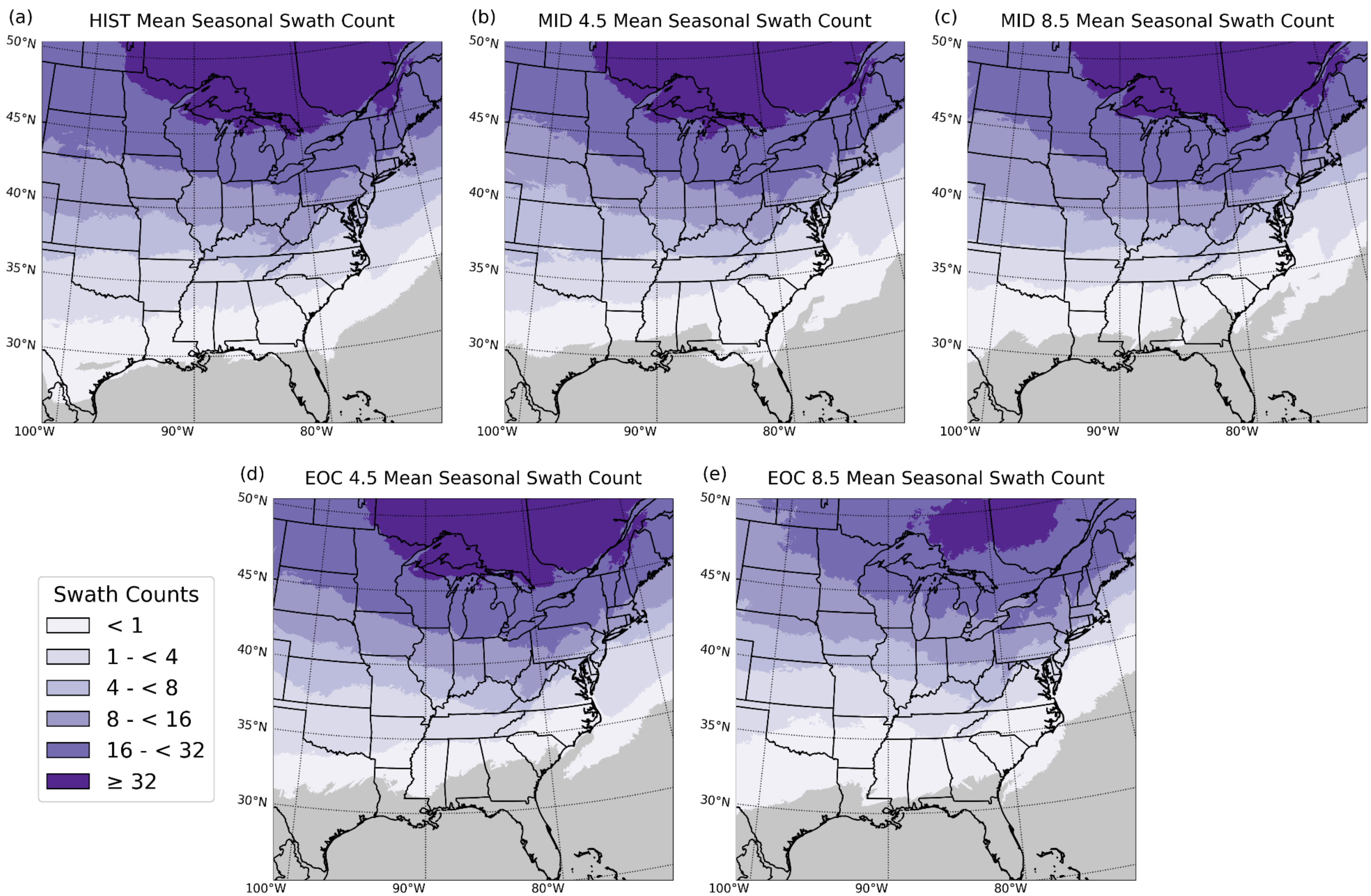

Figure 1. Snowstorm frequency as represented by mean annual swath counts for a) HIST, b) MID4.5, c) MID8.5, d) EOC4.5, and e) EOC8.5. The areas in grey experienced no qualifying swaths during the study period.

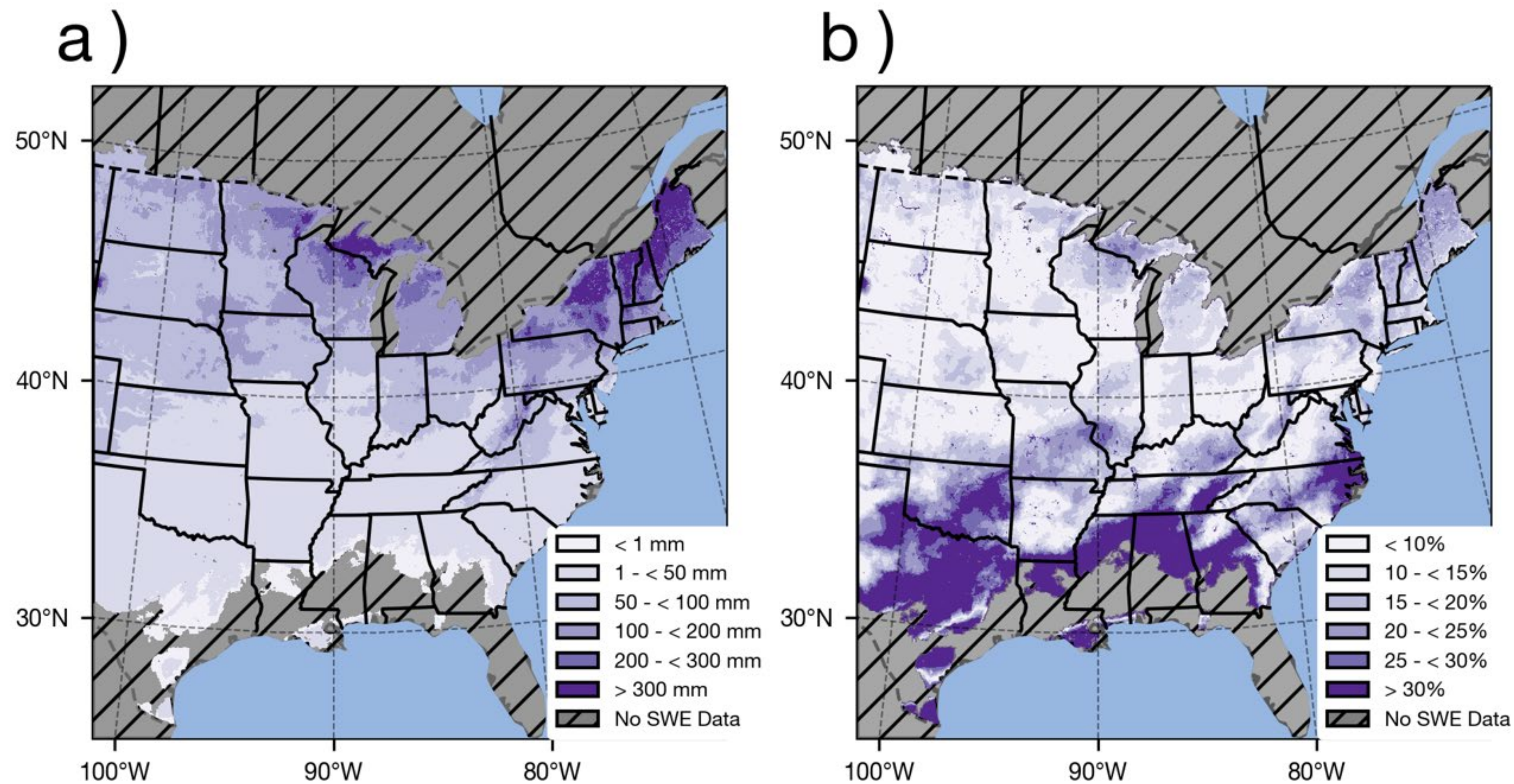

Figure 2. a) October 1 – April 1 2003–2013 SNODAS mean SWE (mm) and b) the percent difference between WRF-BCC HIST (1990–2005) and SNODAS October 1 – April 1 mean SWE. Hatched areas on both figures indicate locations where SNODAS data were not available or both WRF-BCC HIST and SNODAS did not record any SWE.

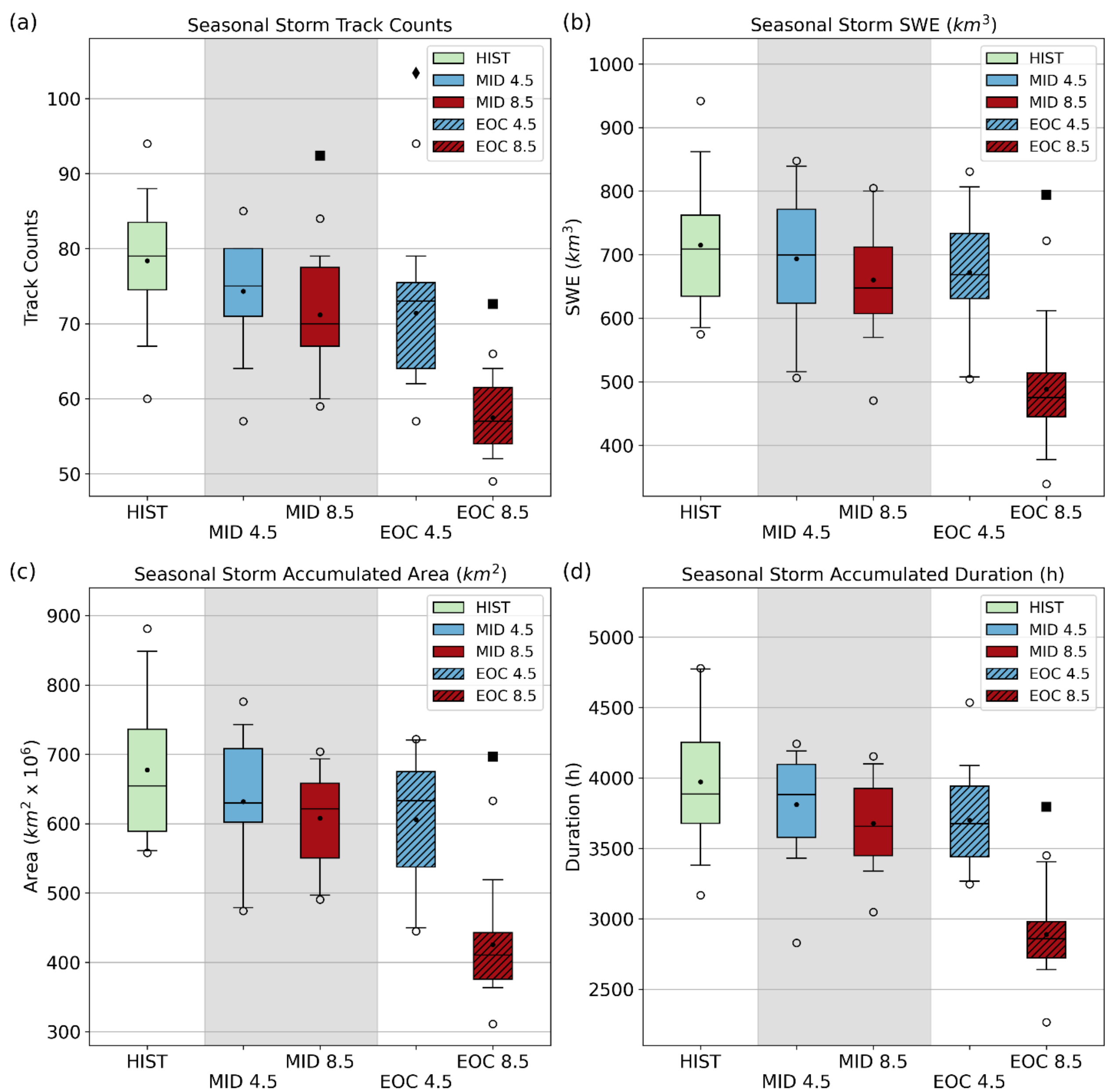

Figure 3. Box-and-whisker plots revealing seasonal comparisons between HIST, MID4.5, MID8.5, EOC4.5, and EOC8.5. Seasonal variability over the study period for select snowstorm swath statistics: a) total counts, b) SWE accumulation, c) storm accumulated area, and d) sum of durations. Means are denoted by black dots and medians are denoted by the black lines. The boxes illustrate the interquartile range, the whiskers represent the 5th and 95th percentiles, and the clear circles denote outliers. Significant differences (using Mann-Whitney U at 95% confidence level) between epochs are identified as squares (diamonds) for differences between HIST and RCP8.5 (RCP4.5).

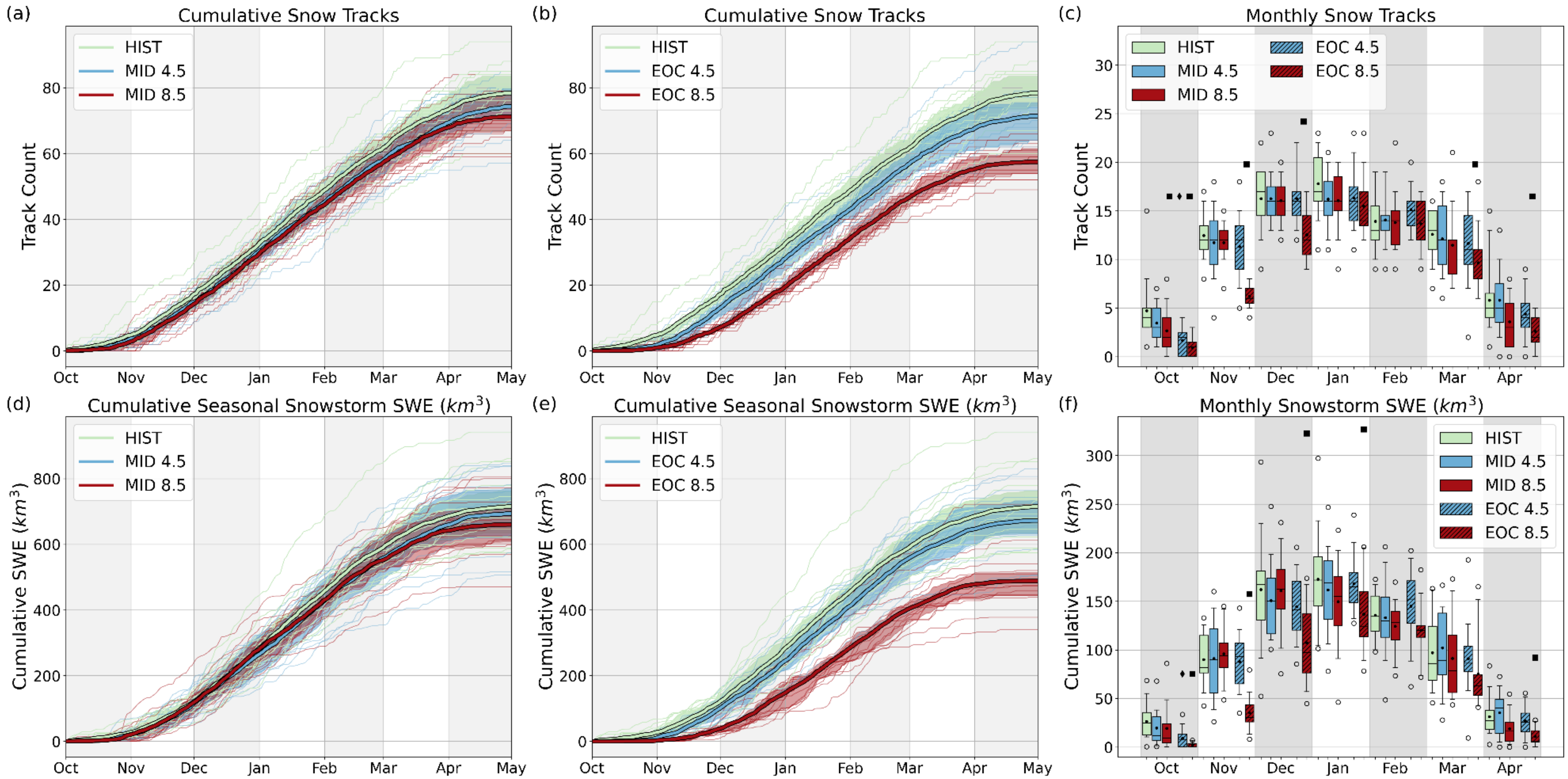

Figure 4. Cumulative frequency diagrams of snowstorm event counts for a) HIST, MID4.5, and MID8.5 and b) HIST, EOC4.5, and EOC8.5 and cumulative seasonal snowstorm SWE (in km3) for d) HIST, MID4.5, and MID8.5 and e) HIST, EOC4.5, and EOC8.5. c) and f) represent box-and-whiskers of monthly snow event counts and monthly snowstorm SWE, respectively. Box-and-whisker detail and significance test labeling as in Figure 3.

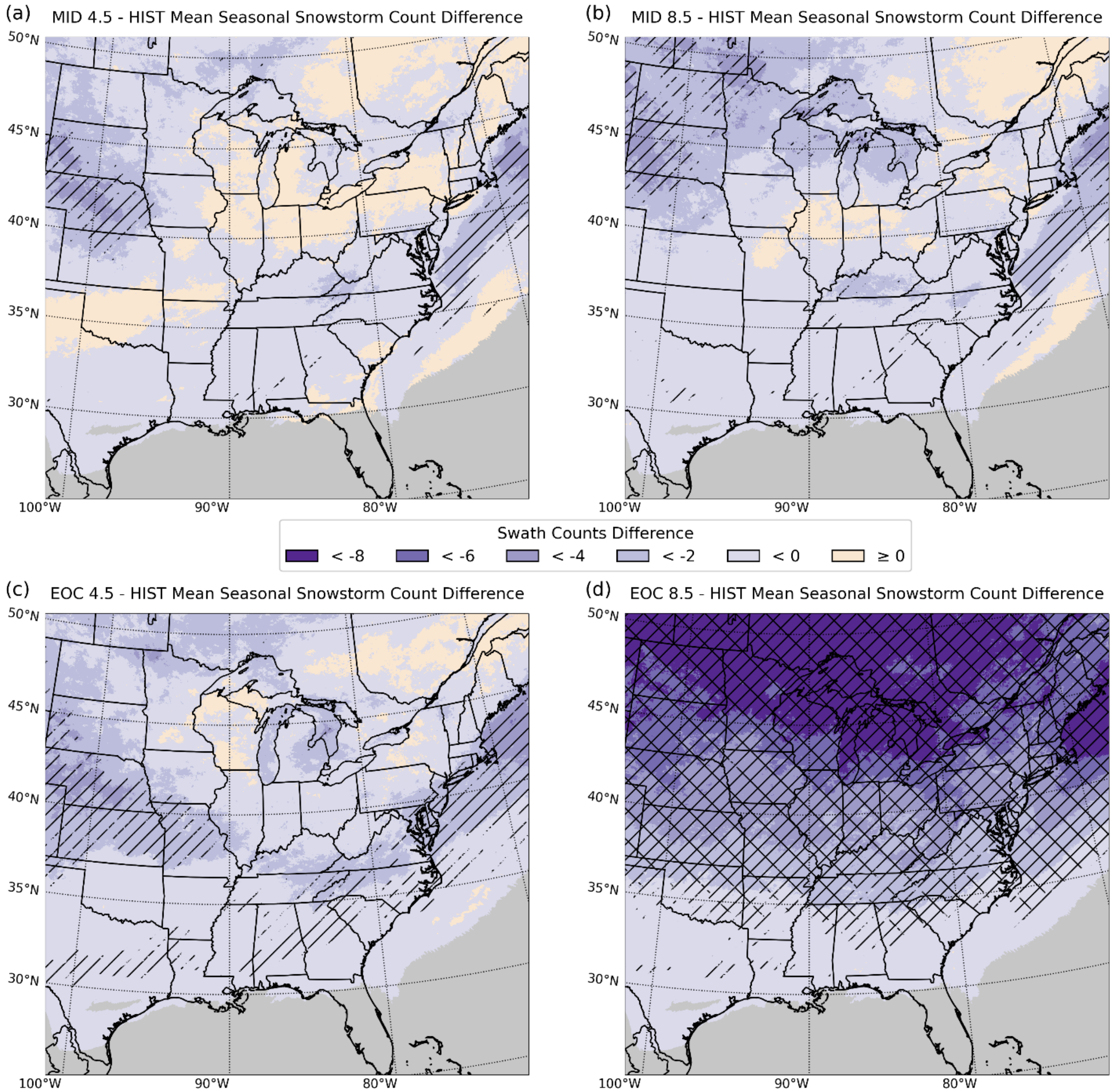

Figure 5. Differences in snowstorm frequency as represented by mean annual swath count difference for a) MID4.5 vs. HIST, b) MID8.5 vs. HIST, c) EOC4.5 vs. HIST, and d) EOC8.5 vs. HIST. Areas in grey experienced no qualifying swaths during the study period. Stippling indicates statistical significance at the 95% confidence level using a Mann–Whitney U test for the medians; double hatched is significant with implementation of a field significance false discovery rate of $\alpha = 0.1$.

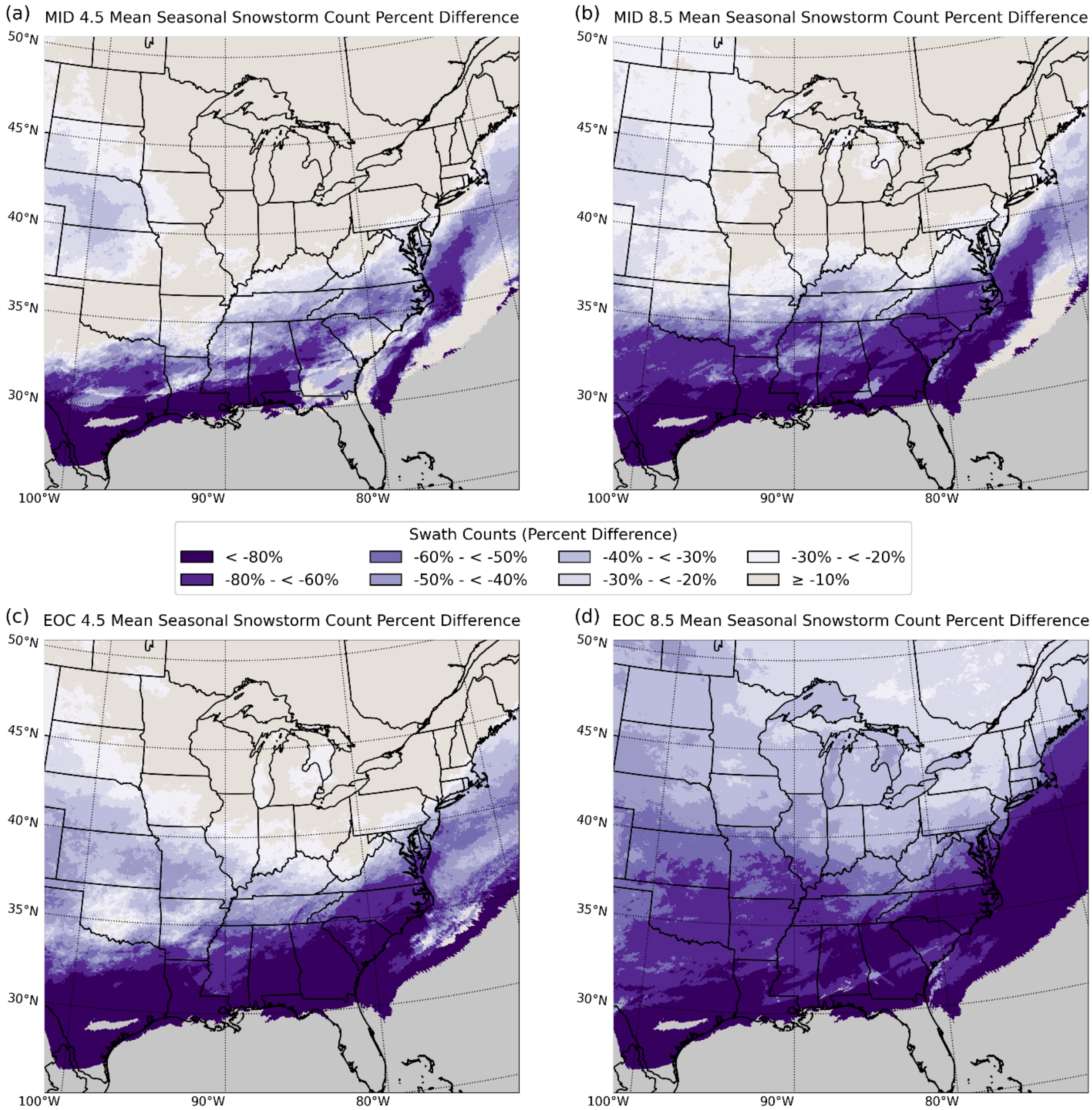

Figure 6. Differences in snowstorm frequency as represented by mean annual swath count percent difference between a) MID4.5 and HIST, b) MID8.5 and HIST, c) EOC4.5 and HIST, and d) EOC8.5 and HIST. The areas in grey experienced no qualifying swaths during the study period.

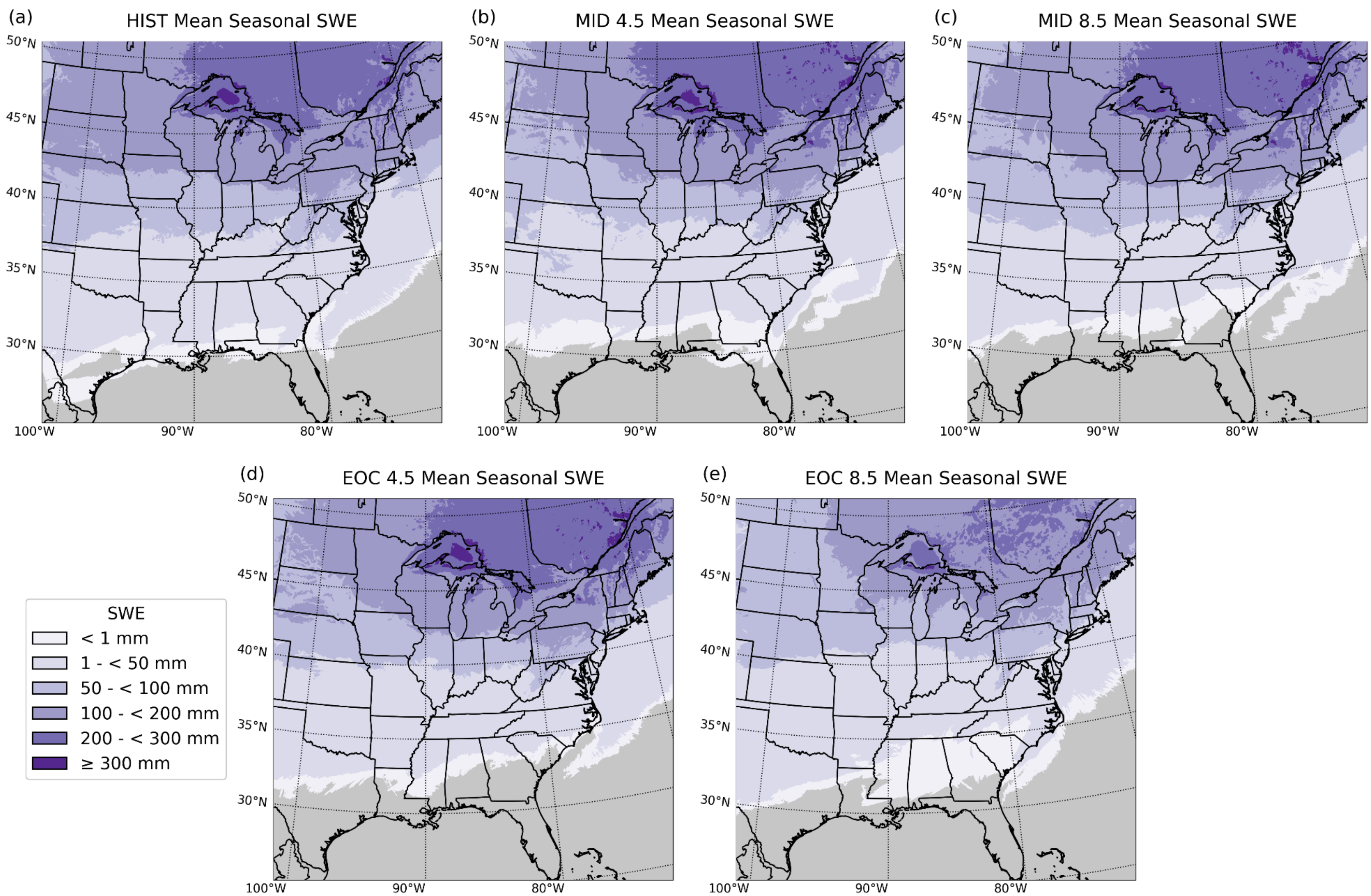

Figure 7. As in Figure 1, except for mean annual snowstorm SWE.

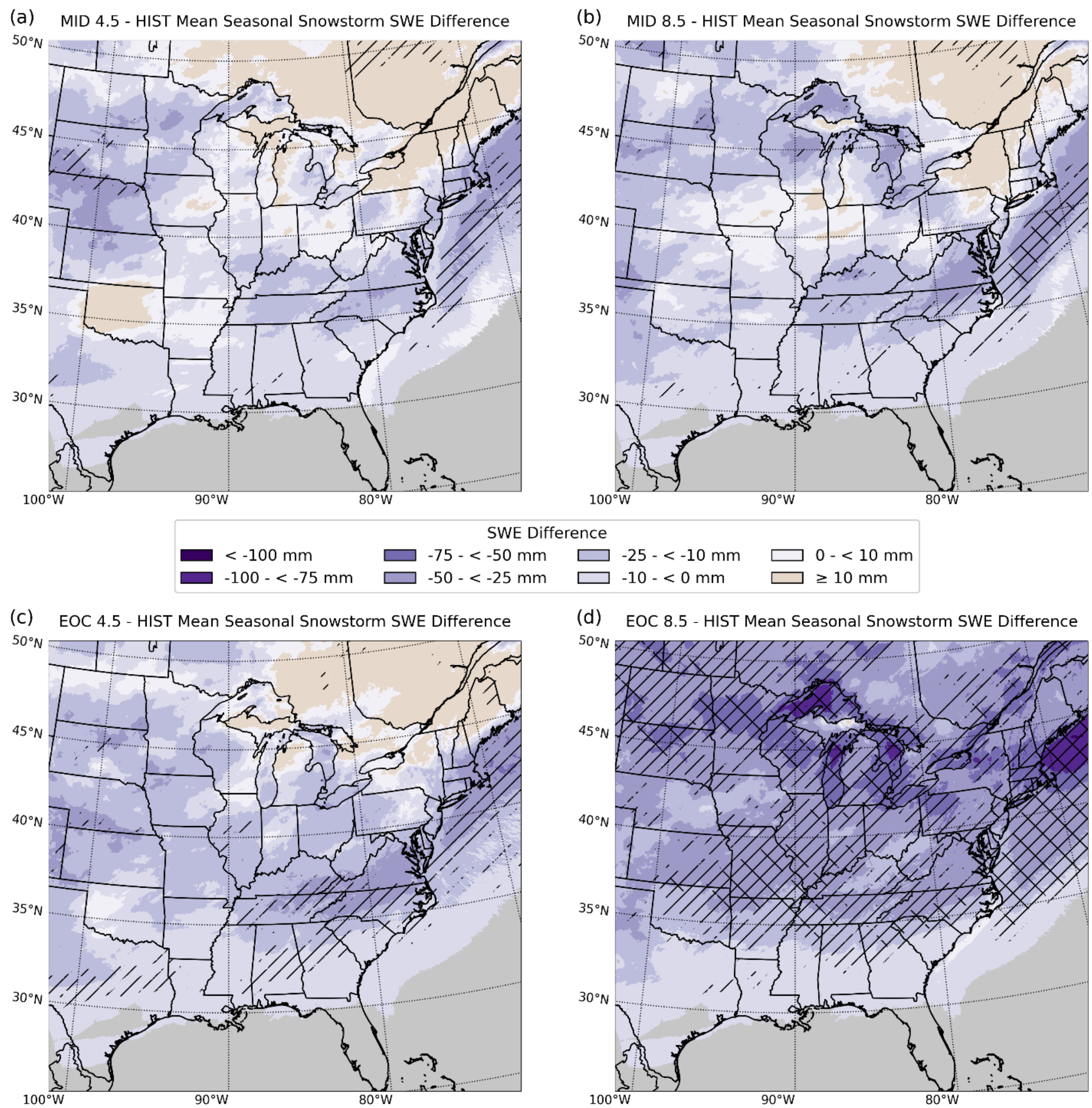

Figure 8. As in Figure 5, except for mean annual snowstorm SWE difference.

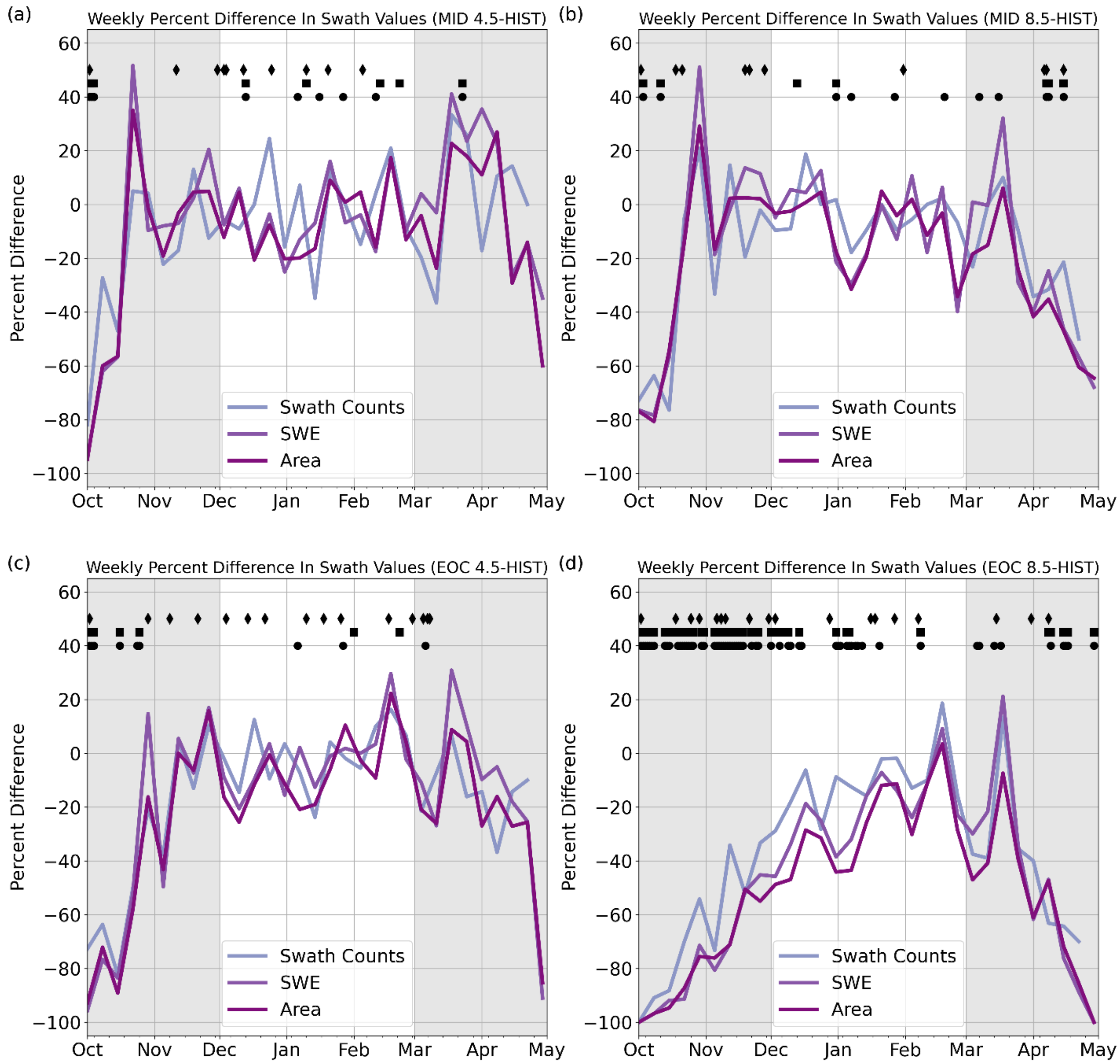

Figure 9. Weekly percent difference for snowstorm metrics between HIST and a) MID4.5, b) MID8.5, c) EOC4.5, and d) EOC8.5. Weekly significantly different (using Mann-Whitney U at 95% confidence level) percent changes between epochs are labeled for swath count (diamonds), SWE (squares), and area (circles).

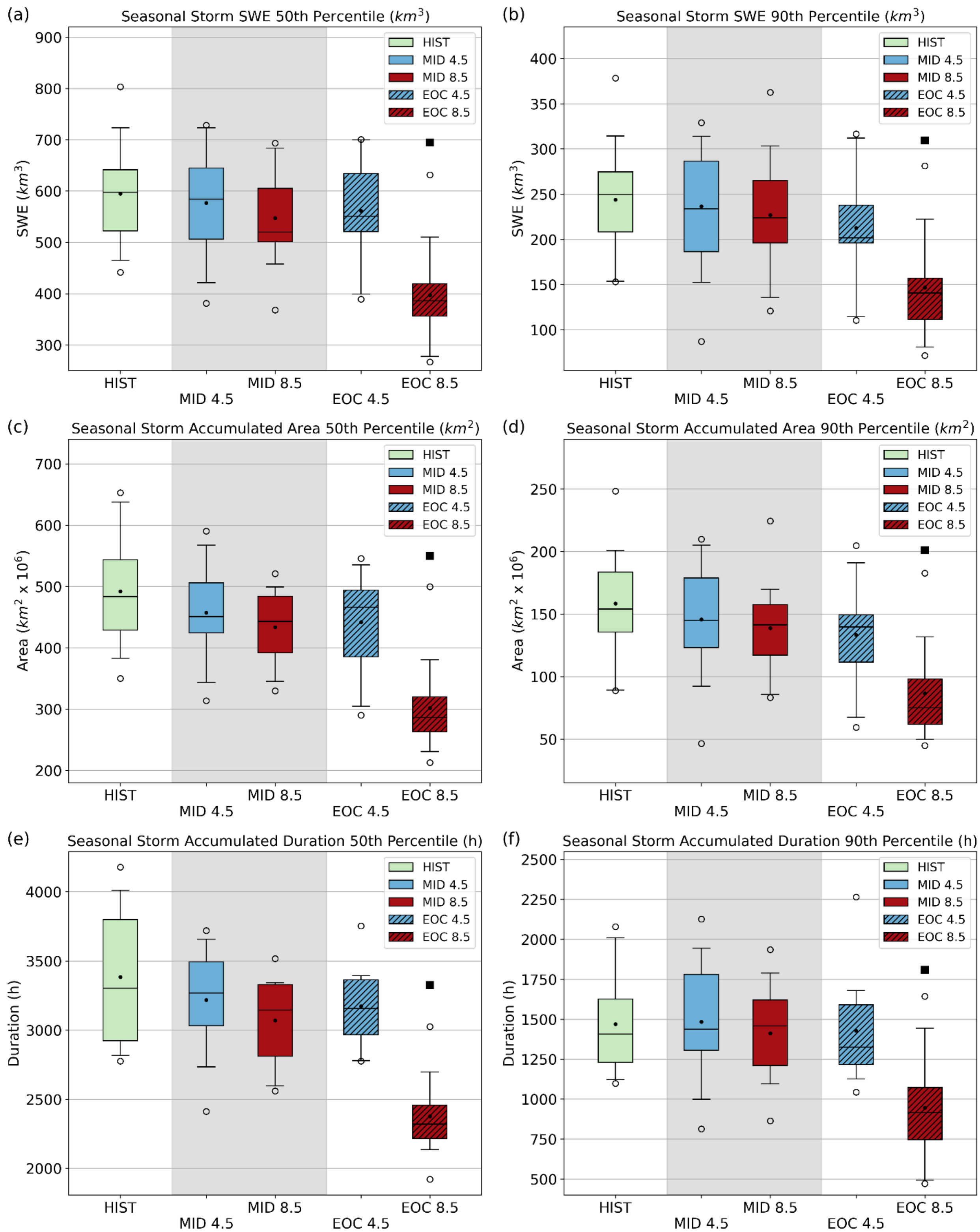

Figure 10. Box-and-whisker plots revealing seasonal comparisons between HIST, MID4.5, MID8.5, EOC4.5, and EOC8.5 for 50th (left) and 90th (right) percentile snowstorm attributes, including SWE (top), accumulated area (middle) and duration (bottom). Both event accumulated area and duration are based on 50th and 90th SWE. Box-and-whiskers and significance testing as in Figure 3.

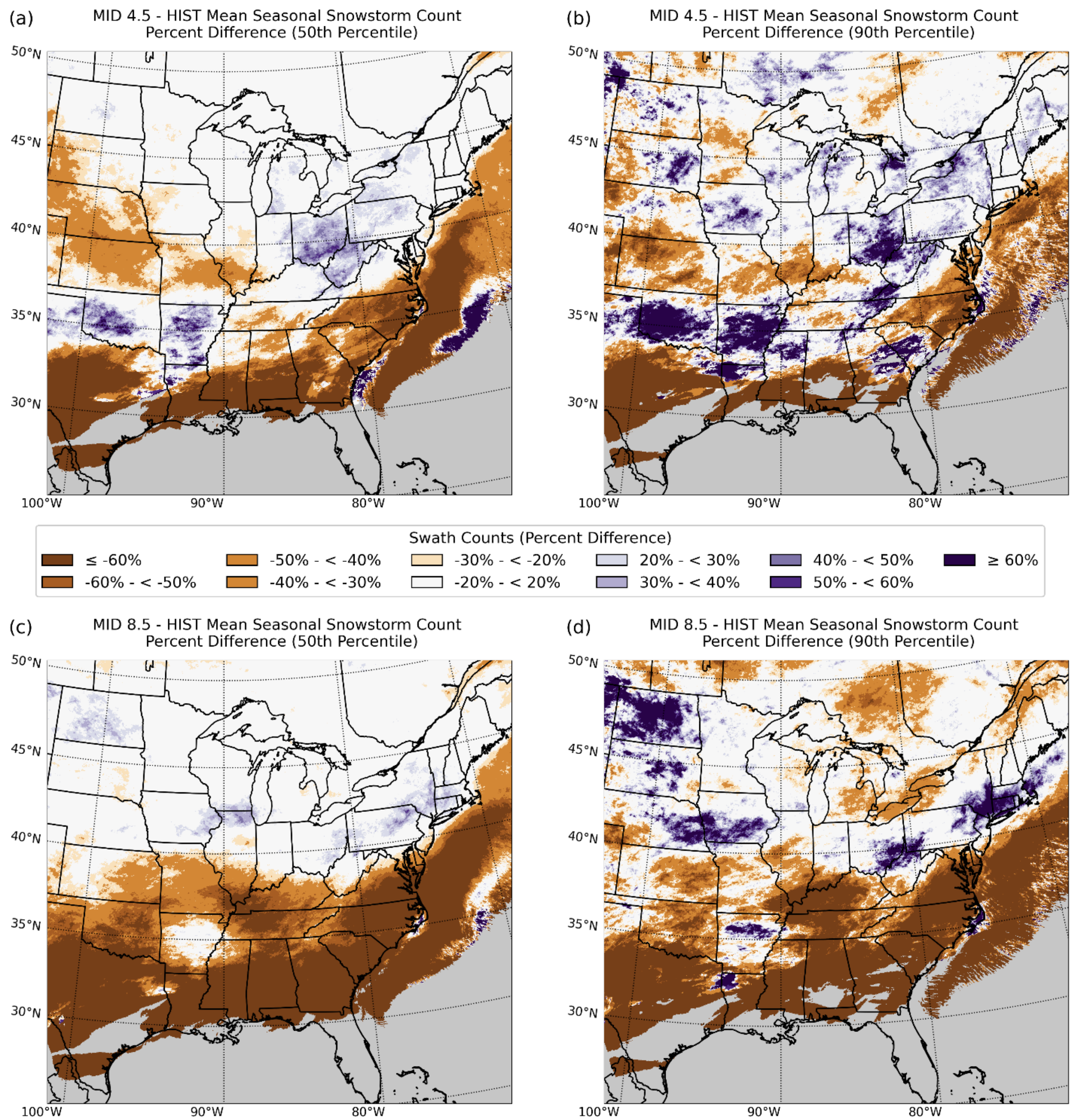

Figure 11. Differences in 50th and 90th percentile snowstorm events as represented by mean annual 50th and 90th percentile swath count percent difference between a) MID4.5 and HIST at 50th percentile, b) MID4.5 and HIST at 90th percentile, c) MID8.5 and HIST at 50th percentile, and d) MID8.5 and HIST at 90th percentile. The areas in grey experienced no qualifying swaths during the study period.

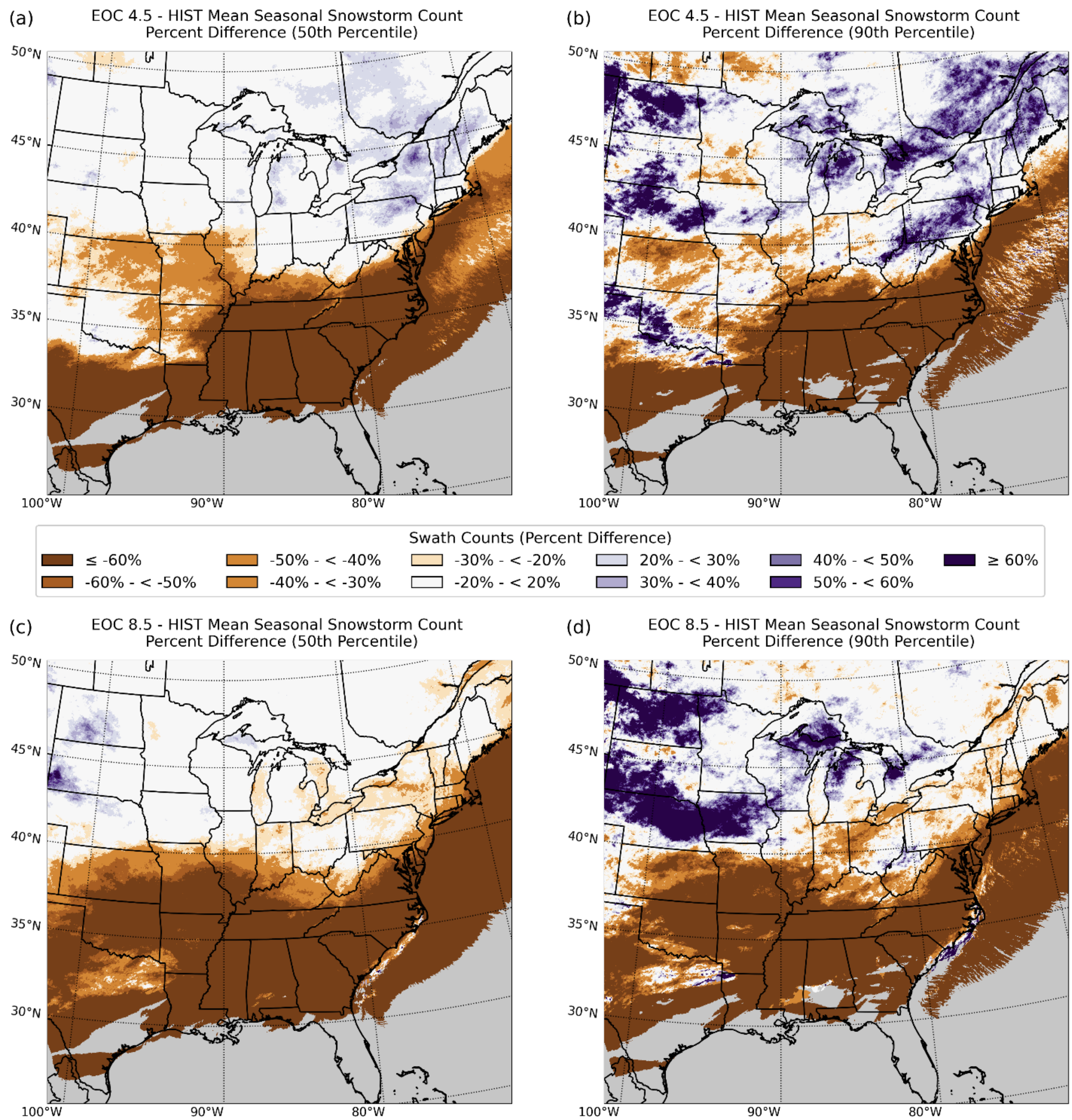

Figure 12. As in Figure 11, except for EOC vs. HIST.

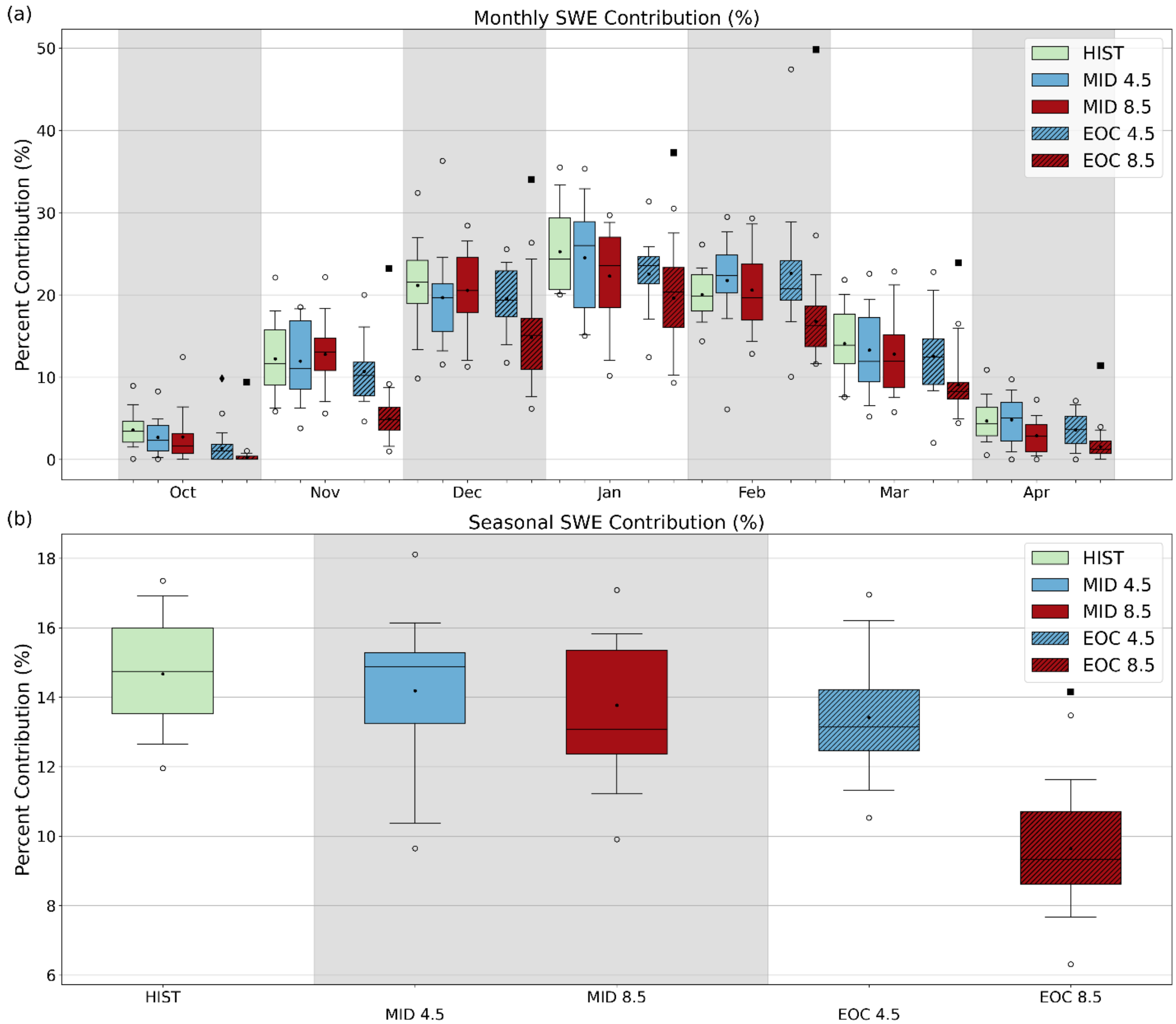

Figure 13. a) Monthly percent contributions of SWE to total precipitation across the domain for all epochs and b) total seasonal (Oct-Apr) contributions of SWE to total precipitation for all epochs. Box-and-whiskers and significance testing as in Figure 3.

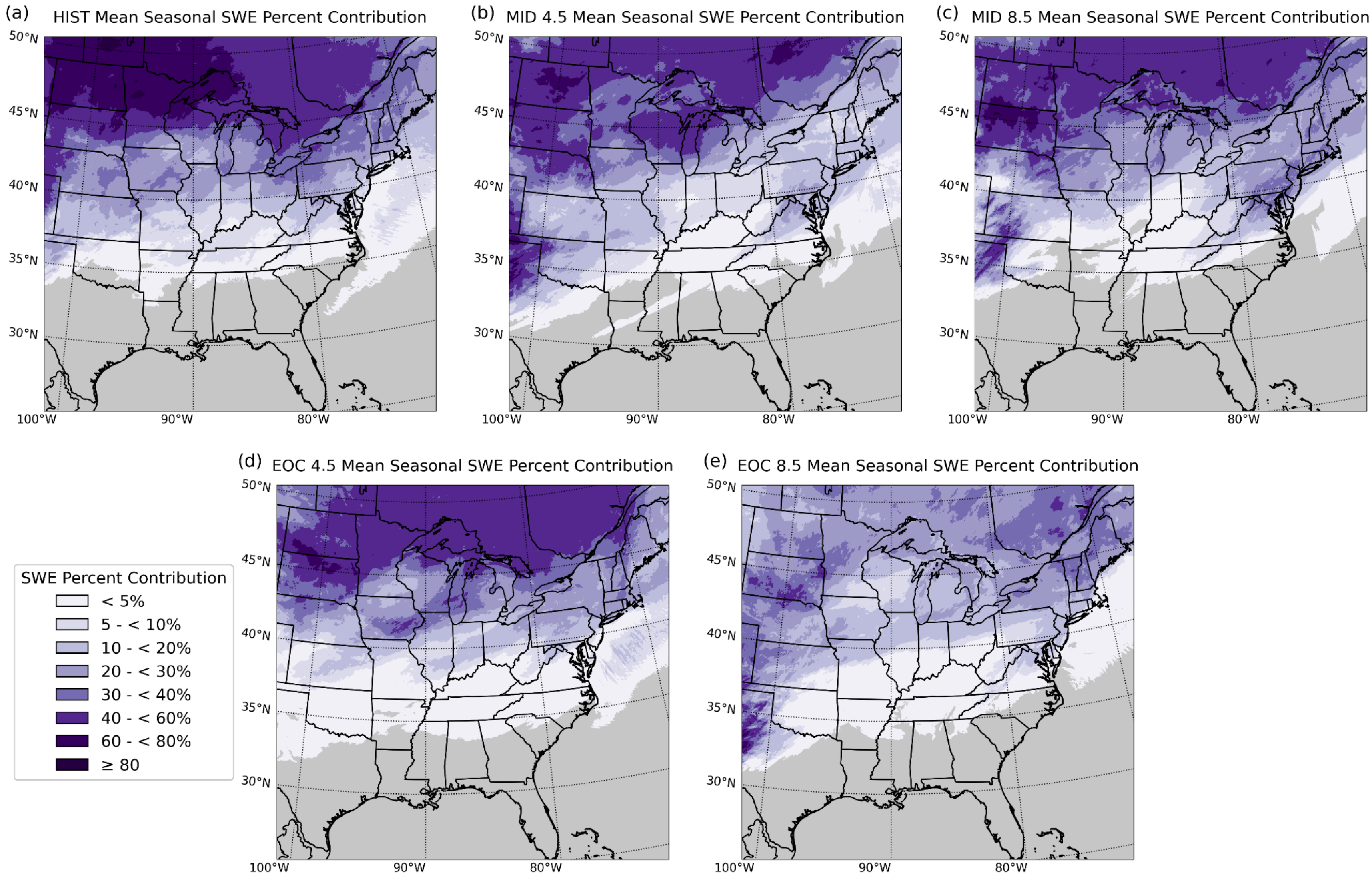

Figure 14. As in Figure 1, except for mean seasonal SWE percent contribution to total precipitation.

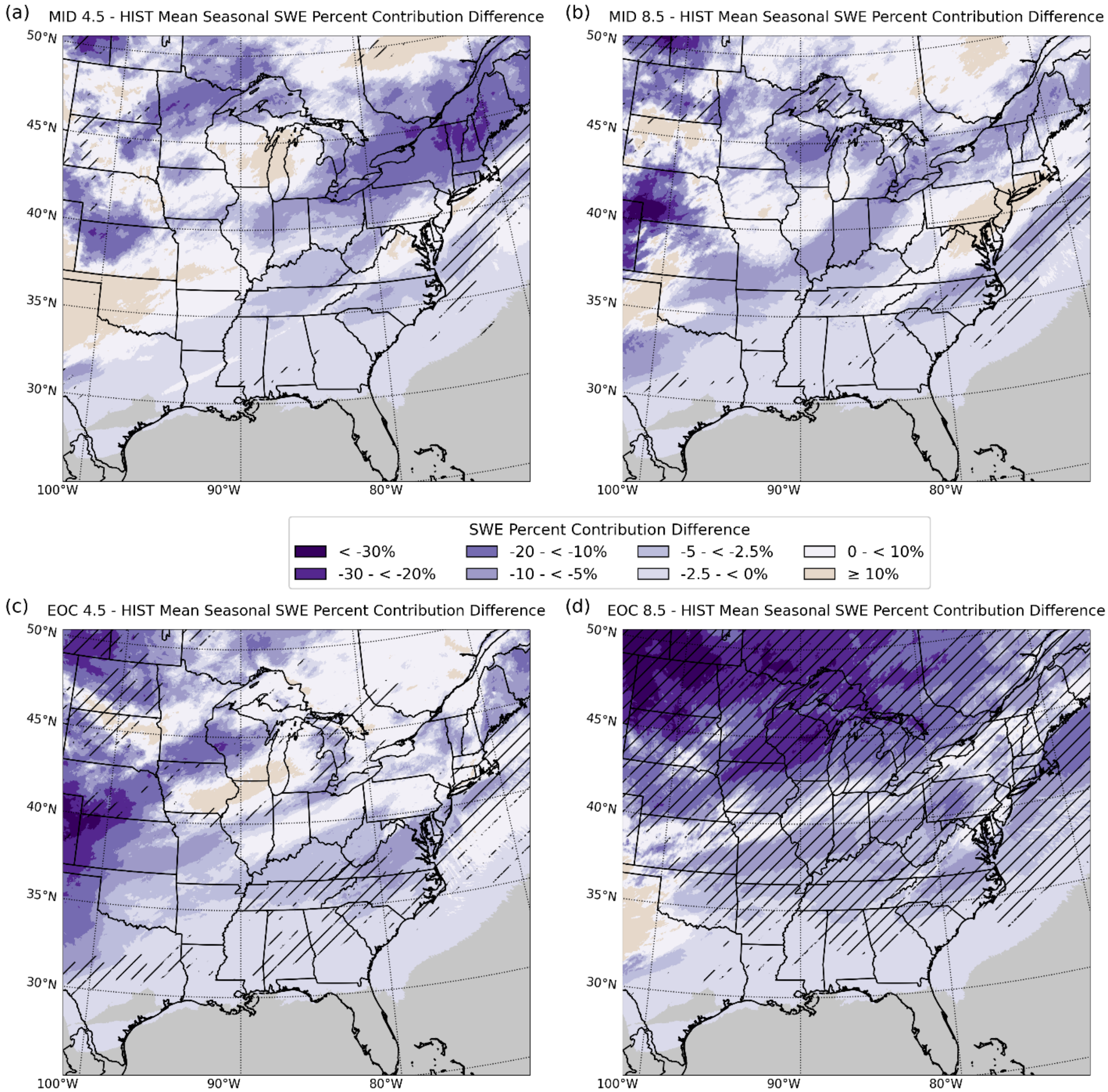

Figure 15. As in Figure 5, except for snow contribution to total seasonal precipitation.

Figure legends

Figure 1. Snowstorm frequency as represented by mean annual swath counts for a) HIST, b) MID4.5, c) MID8.5, d) EOC4.5, and e) EOC8.5. The areas in grey experienced no qualifying swaths during the study period.

Figure 2. a) October 1 – April 1 2003–2013 SNODAS mean SWE (mm) and b) the absolute difference between WRF-BCC HIST (1990–2005) and SNODAS mean for October 1 – April 1 SWE shown as a percent of the total mean SNODAS SWE. Hatched areas on both figures indicate locations where SNODAS data were not available or both WRF-BCC HIST and SNODAS did not record any SWE.

Figure 3. Box-and-whisker plots revealing seasonal comparisons between HIST, MID4.5, MID8.5, EOC4.5, and EOC8.5. Seasonal variability over the study period for select snowstorm swath statistics: a) total counts, b) SWE accumulation, c) storm accumulated area, and d) sum of durations. Means are denoted by black dots and medians are denoted by the black lines. The boxes illustrate the interquartile range, the whiskers represent the 5th and 95th percentiles, and the clear circles denote outliers. Significant differences (using Mann-Whitney U at 95% confidence level) between epochs are identified as squares (diamonds) for differences between HIST and RCP8.5 (RCP4.5).

Figure 4. Cumulative frequency diagrams of snowstorm event counts for a) HIST, MID4.5, and MID8.5 and b) HIST, EOC4.5, and EOC8.5 and cumulative seasonal snowstorm SWE (in km3) for d) HIST, MID4.5, and MID8.5 and e) HIST, EOC4.5, and EOC8.5. c) and f) represent box-and-whiskers of monthly snow event counts and monthly snowstorm SWE, respectively. Box-and-whisker detail and significance test labeling as in Figure 3.

Figure 5. Differences in snowstorm frequency as represented by mean annual swath count difference for a) MID4.5 vs. HIST, b) MID8.5 vs. HIST, c) EOC4.5 vs. HIST, and d) EOC8.5 vs. HIST. Areas in grey experienced no qualifying swaths during the study period. Stippling indicates statistical significance at the 95% confidence level using a Mann–Whitney U test for the medians; double hatched is significant with implementation of a field significance false discovery rate of $\alpha = 0.1$.

Figure 6. Differences in snowstorm frequency as represented by mean annual swath count percent difference between a) MID4.5 and HIST, b) MID8.5 and HIST, c) EOC4.5 and HIST, and d) EOC8.5 and HIST. The areas in grey experienced no qualifying swaths during the study period.

Figure 7. As in Figure 1, except for mean annual snowstorm SWE.

Figure 8. As in Figure 5, except for mean annual snowstorm SWE difference.

Figure 9. Weekly percent difference for snowstorm metrics between HIST and a) MID4.5, b) MID8.5, c) EOC4.5, and d) EOC8.5. Weekly significantly different (using Mann-Whitney U at 95% confidence level) percent changes between epochs are labeled for swath count (diamonds), SWE (squares), and area (circles).

Figure 10. Box-and-whisker plots revealing seasonal comparisons between HIST, MID4.5, MID8.5, EOC4.5, and EOC8.5 for 50th (left) and 90th (right) percentile snowstorm attributes, including SWE (top), accumulated area (middle) and duration (bottom). Both event accumulated area and duration are based on 50th and 90th SWE. Box-and-whiskers and significance testing as in Figure 3.

Figure 11. Differences in 50th and 90th percentile snowstorm events as represented by mean annual 50th and 90th percentile swath count percent difference between a) MID4.5 and HIST at 50th percentile, b) MID4.5 and HIST at 90th percentile, c) MID8.5 and HIST at 50th percentile, and d) MID8.5 and HIST at 90th percentile. The areas in grey experienced no qualifying swaths during the study period.

Figure 12. As in Figure 11, except for EOC vs. HIST.

Figure 13. a) Monthly percent contributions of SWE to total precipitation across the domain for all epochs and b) total seasonal (Oct-Apr) contributions of SWE to total precipitation for all epochs. Box-and-whiskers and significance testing as in Figure 3.

Figure 14. As in Figure 1, except for mean seasonal SWE percent contribution to total precipitation.

Figure 15. As in Figure 5, except for snow contribution to total seasonal precipitation.

Graphical Abstract

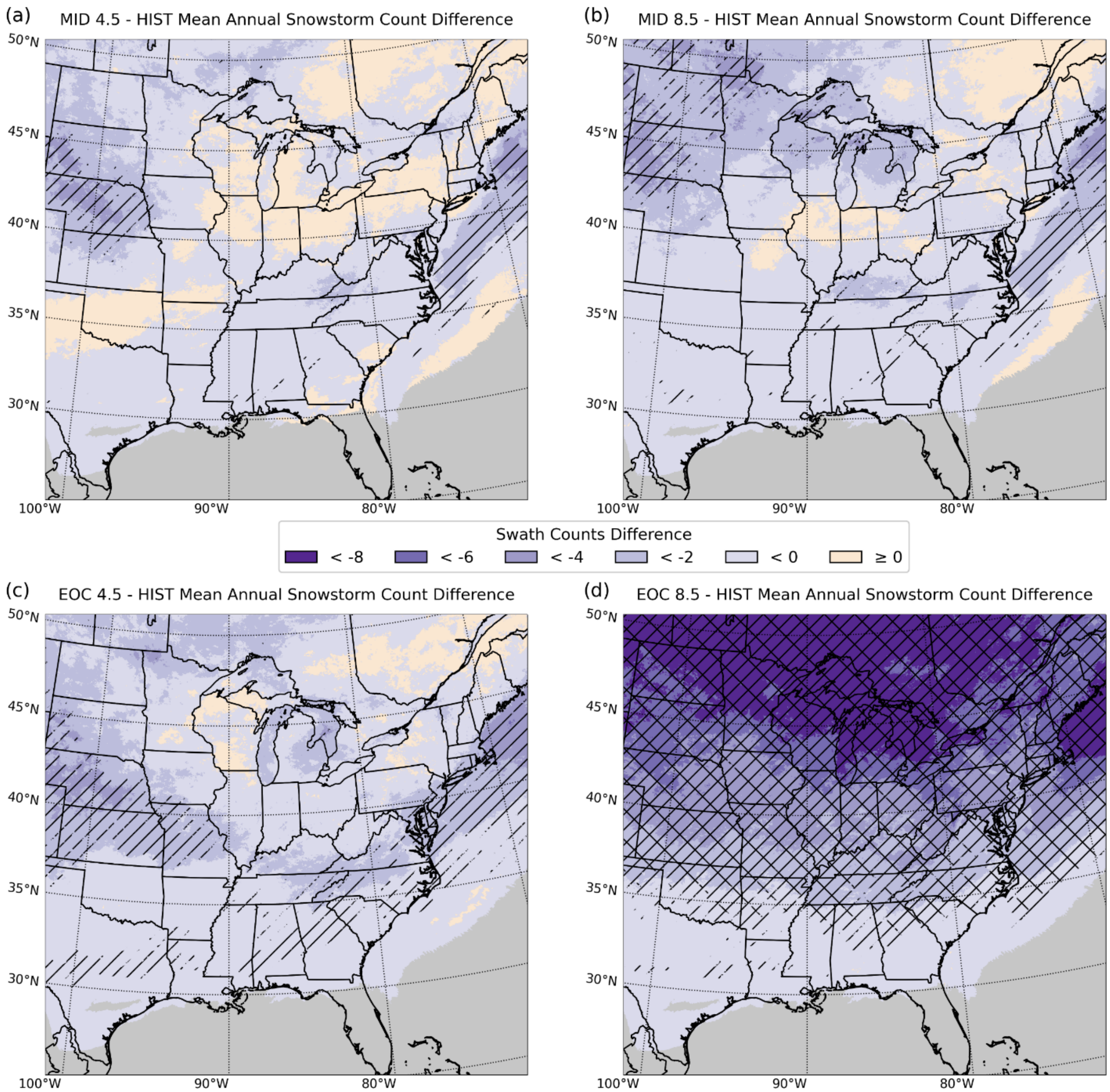

Title: The Future of Snowstorms in Central and Eastern North America

Authors: Walker S. Ashley*, Aaron Zeeb, Alex M. Haberlie, Vittorio A. Gensini, and Allison Michaelis

80-word Statement: The frequency, placement, and intensity of snowstorms are projected to change across North America during the twenty-first century. Changes are most dramatic for the pessimistic climate pathway, where significant declines are projected for various snowstorm attributes, including frequency, SWE, area, and duration. The two most notable future changes are the significant declines in shoulder season snowstorms and the poleward shift in the latitude that demarcates steady snowstorm counts to the north and reduced, or elimination of, snowstorms to the south.